STABILITY ANALYSIS OF GENERALIZED
CELLULAR NEURAL NETWORKS

by

Cuneyt Guzelis and Leon O. Chua

STABILITY ANALYSIS OF GENERALIZED
CELLULAR NEURAL NETWORKS

by

Cuneyt Guzelis and Leon O. Chua

Memorandum No. UCB/ERL M91/23

15 March 1991

ELECTRONICS RESEARCH LABORATORY

College of Engineering
University of California, Berkeley
94720

STABILITY ANALYSIS OF GENERALIZED
CELLULAR NEURAL NETWORKS

by

Cuneyt Guzelis and Leon O. Chua

ELECTRONICS RESEARCH LABORATORY

College of Engineering
University of California, Berkeley
94720

STABILITY ANALYSIS OF
GENERALIZED CELLULAR NEURAL NETWORKS †

Cuneyt Guzelis   and   Leon O. Chua † †

ABSTRACT

A rather general class of neural networks, called generalized Cellular Neural Networks (CNNs), is introduced. The new model covers most of the known neural network architectures including Cellular Neural Networks, Hopfield Networks and Multi-layer Perceptrons. Several sets of conditions, ensuring the input-output stability and global asymptotic stability of generalized CNNs, have been obtained. The conditions for the stability of individual cells are checked in the frequency domain, while the stability of the overall network is analyzed in terms of the stability of the individual cells and the connectivity characteristics. The results on the global asymptotic stability are useful for the design of a generalized CNN such that the orbit of each state converges to a globally asymptotically stable equilibrium point which depends only on the input and not on the initial state. Such a network defines an algebraic map from the space of external inputs to the space of steady-state values of the outputs, and hence, can accomplish cognitive and computational tasks.

† † C. Guzelis is with the Faculty of Electrical-Electronics Engineering, Istanbul Technical University, Maslak 80626, TURKEY.

L. O. Chua is with the Department of Electrical Engineering and Computer Sciences, University of California, Berkeley, CA 94720.

I. INTRODUCTION

In the past three decades, a number of neural network architectures has been developed. The architectures have been inspired both by the principles governing biological neural systems and the well-established theories of engineering and fundamental sciences. Most of the widely applied neural networks fall into two main classes: 1) Memoryless Neural Networks [5], and 2) Dynamical Neural Networks [1], [3], [4], [6]. From a circuit theoretical point of view, the Memoryless Neural Networks are nonlinear resistive circuits, while the Dynamical Neural Networks are nonlinear R-L-C circuits. A Memoryless Neural Network defines a nonlinear transformation from the space of input signals into the space of output signals. Such networks have been successfully used in pattern recognition and several problems which can be defined as a nonlinear transformation between two spaces. As in Hopfield Network (HN) [4] and Cellular Neural Network (CNN) [1], the Dynamical Neural Networks have been usually designed as dynamical systems where the inputs are set to some constant values, and each trajectory approaches one of the stable equilibrium points depending upon the initial state. Some useful applications of these networks includes image processing, pattern recognition and optimization.

This paper presents a new neural network architecture, called generalized Cellular Neural Network (CNN), which is a generalization of CNN introduced in [1]. The generalized CNN includes, as special cases, some important Memoryless Networks, such as Multilayer Perceptrons (MPs), and Dynamical Networks, such as HN and CNN. A generalized CNN is an interconnection of many subcircuits, called cells, each of which is an arbitrary order dynamical circuit and is connected only to its nearest neighbors. High order generalized CNNs are capable of more functions than the neural networks made up of simple R-C op amp cells.

The development of generalized CNN has been influenced by the following facts: i) Neurobiological studies have demonstrated that neurons exhibit quite complicated dynamical behaviours [6], and therefore should be considered as an analog microprocessor rather than as a simple processing element; ii) The set of differential-difference equations (1)-(4), describing the generalized CNN, defines a rather general class of nonlinear equations. Indeed, most of the equations governing nonlinear circuits and systems fall into this important class [11], [19]; and a partial linearization of nonlinear differential equations hav-

ing the state equation form also yields such a class of nonlinear equations [7]. Moreover, any system defined by this class of nonlinear equations can be considered as a feedback control system for which many comprehensive results have been obtained in the literature [7]-[9]; and iii) The generalized CNN covers many important neural network architectures as special cases. For instance, the MP is a 0 th order generalized CNN while the HN and the CNN are 1 st order generalized CNNs. Consequently, a generalized CNN is capable of performing any task that these special networks can perform, while it offers more capability than these networks.

In the design of a Dynamical Neural Network, it is always of interest to study the stability properties of the network. The vast majority of the stability studies in neural networks [1]-[4], [12], [14]-[15] has been devoted to finding the conditions which ensure that each trajectory of the network converges to an equilibrium point depending on the initial conditions. These completely stable neural networks have been used as computing and/or cognitive machines. Here, the external inputs are set to some constant values, the input data is fed via initial conditions, and the outputs take their steady-state values at an equilibrium point that depends on the initial condition. Such neural networks can accomplish many tasks, such as pattern recognition and image processing [1], [3]-[4], [13].

In contrast with the Dynamical Neural Networks mentioned above, one can design a Dynamical Neural Network where the input data is fed via external inputs, and each trajectory converges to a unique equilibrium point that depends only on the input and not on the initial state. Such a globally asymptotically stable neural network has been presented in [10]. The neural network, designed in this way, defines an algebraic transformation from the space of inputs into the space of steady-state outputs. Therefore, it can perform computational and cognitive tasks. In this paper, we present several sets of sufficient conditions for global asymptotic stability, and also for input-output stability of generalized CNN. The global asymptotic stability results are useful for the design of a generalized CNN where the output reaches its steady-state value depending only on the given constant input and not on the initial state. The input-output stability results can be used for determining the boundedness of the outputs of a generalized CNN with constant inputs, as well as for a generalized CNN with time-varying inputs.

The organization of this paper is as follows. In section II, we describe the connection topology of

the generalized CNN, the circuit structure of the cells, and the building blocks of generalized CNN. In section III, a set of sufficient conditions for the global asymptotic stability and input-output stability of the individual cells, is given and it is shown by some concrete examples that the dynamical behaviours of the cells are much richer than those of simple cells of common neural networks. The stability results presented in section III are based on the circle criterion of control theory, and they will be exploited, in section IV, to develop the conditions for the whole generalized CNN. Section IV presents some results on the existence, uniqueness and boundedness of the trajectories of generalized CNN, and two types of conditions ensuring the input-output stability and global asymptotic stability of a rather general class of generalized CNN. The first type of conditions are applied to the whole generalized CNN and do not exploit the stability of the individual cells. The second type of conditions are in terms of the connection topology, the connection weights and the frequency domain transfer function of the linear subcircuit of individual cells. The conditions can be checked only in the frequency domain and verified by a kind of Nyquist graphical test.

II. GENERALIZED CNN

In this section, a rather general class of neural networks, called generalized Cellular Neural Networks , is presented. A generalized CNN is a large-scale nonlinear circuit composed of a large number of subcircuits, called cells. Each cell is an arbitrary order dynamical circuit and is connected only to its nearest neighbors (the term nearest will be clarified in Definition 1).

Connection Topology :

A row of N_1 cells is called a 1-dimensional single-layer generalized CNN and denoted by Π^1 . An $N_1 \times N_2$ array of cells is called a 2-dimensional single layer generalized CNN, and denoted by Π^2 . Similarly, an n-dimensional single-layer generalized CNN, Π^n , is an $N_1 \times N_2 \cdots \times N_n$ array of cells; here each N_j is an integer number. An n-dimensional m-layer generalized CNN, Ω_m^n , is built-up from a collection of m single-layer generalized CNNs Π_k^n , $k \in \{1,2,...,m\}$, in such a way that the cells in each layer Π_k^n are connected to the nearest neighbors in the other layers Π_j^n , $j \neq k$. By the existence of a connection between two cells, we mean that the output of one of the cells is fed into the

other. If each of these two cells is fed by the output of the other, the connection is called bilateral; otherwise, it is unilateral. In our illustrations, a link without an orientation will denote a connection which may be unilateral or bilateral, while a link with an orientation will denote a unilateral connection. A bilateral connection will be denoted by two oriented links.

A 2-dimensional 3-layer generalized CNN, Ω_3^2 , is shown in Figure 1. The layer Π_1^2 , Π_2^2 ,and respectively Π_3^2 is a 3×3 , 4×3 , and respectively 3×5 array of cells. As in the generalized CNN of Figure 1, the size ($N_j's$) and the connection topology may, in general, differ from one layer to another. Moreover, a layer may be rectangular array of cells, i.e., $N_1 \neq N_2$. For simplicity, however, unless otherwise stated, we will assume that the size of each layer is the same, i.e. , $N_j^k = N_j$ for all $j \in \{ 1,2,...,n \in$ and $k \in \{ 1,2,...,m \}$, where the superscript k index the layers. Note that a typical cell (say, the hatched cell in Π_2^2) in Figure 1 is connected not only to its nearest neighbors in the same layer, but also to the nearest neighbors in the upper (except the uppermost layer) and the lower (except the lowermost layer) layers. For the sake of generality, we allow the "size" of the neighborhood in each layer to be arbitrary, including the entire layer. Moreover, in the most general case, each cell of each layer may be connected to the cells in more than 2 layers. Using future technologies, such as optical systems, such interconnections are feasible.

Figure 1

A special class of layered generalized CNN is feedforward generalized CNN, Γ_m^n , inwhich the output of the cells in a layer Π_k^n is fed only into the cells in the next layer Π_{k+1}^n . The cells within the same layer are connected to their nearest neighbors as before. A generalization of a feedforward generalized CNN is a cascade [2], Φ_m^n , where the output of the cells in a layer Π_k^n is fed not only into the cells in the next layer Π_{k+1}^n , but also into the cells in the succeeding layers Π_j^n with $j \in \{ k+2, k+3, \ldots, m \}$. Note that the connections between layers in a cascade are all unilateral whereas the connections within a layer may not be. A generalized CNN is called recurrent, if it has a bilateral connection and/or a loop consisting of similarly directed unilateral connections.

Figure 2a, 2b and 2c shows a feedforward generalized CNN Γ_j^i , a cascade Φ_j^i of cells, and a recurrent generalized CNN, respectively.

Figure 2

A cell in the k th layer of an n-dimensional m-layer generalized CNN will be denoted by $C_{i_1,i_2,\ldots,i_n,k}$ where $i_j \in \{1,2,\ldots,N_j\}$ for all $j \in \{1,2,\ldots,n\}$ and $k \in \{1,2,\ldots,m\}$. For brevity, let us define $i = (i_1,i_2,\ldots,i_n,k)$ and then set $C_{i_1,i_2,\ldots,i_n,k} = C_i$. Sometimes we will still write $C_{i_1,i_2,k}$ and $C_{i,k}$ rather than C_i particularly when $n = 2$ and $n = 1$, respectively. Definition 1 below describes what we mean by a nearest neighbor of a cell.

Definition 1 : For a cell C_i in the k th layer of an n-dimensional m-layer generalized CNN Ω_m^n and a metric † $d_{k,l}(\bullet;\bullet)$ and a positive integer number $r_{k,l}$, the nearest neighborhood $B_{i,l}$ in the l th layer is defined by

$$B_{i,l} = \{ C_{\hat{i}} \mid d_{k,l}(i;\hat{i}) \leq r_{k,l} , i \neq \hat{i} = (\hat{i}_1,\hat{i}_2,\ldots,\hat{i}_n,l) , \hat{i}_j \in \{1,2,\ldots,N_j\}$$
$$\text{for } all \ j \in \{1,2,\ldots,n\} \ \}$$

where $d_{k,l}(i;\hat{i})$ is the distance between the vectors of integer numbers $(i_1,i_2,\ldots,i_n,k)^T$ and $(\hat{i}_1,\hat{i}_2,\ldots,\hat{i}_n,l)^T$. Different metrics may be chosen for $d_{k,l}$. The set of nearest-neighbors of a cell C_i is the union of all nearest-neigborhoods $B_{i,l}$ in the different layers and is denoted by

$$B_i = \bigcup B_{i,l} . \ \square$$

Since each cell is connected only to its nearest neighbors, the connection topology depends on the choice of r and the distance function d only. Note that the nearest neighborhood of a cell may be an empty set in one extreme case, or it may contain all cells of the generalized CNN as in the Hopfield

---

† We define a metric $d_{k,l}(\bullet;\bullet)$ in the usual sense; namely, a $d_{k,l}(\bullet;\bullet)$ is a real-valued function such that the following axioms are satisfied: i) $d_{k,l}(i;\hat{i}) = d_{k,l}(\hat{i};i)$ for all $i,\hat{i}$. ii) $d_{k,l}(i,\hat{i}) \leq d_{k,l}(i,\hat{i}) + d_{k,l}(\hat{i},\hat{i})$ for all $i, \hat{i}, \hat{\hat{i}} = (i_1,i_2,\ldots,i_n,l)$, $i_j \in \{1,2,\ldots,N_j\}$ for all $j \in \{1,2,\ldots,n\}$. iii) $d_{k,l}(i,\hat{i}) > 0$ for all $i \neq \hat{i}$ and $d_{k,l}(i,i) = 0$.

Network [4], in the other extreme case.

In general, we can choose different r and d for each cell, layer and/or pair of layers. This, however, causes a nonuniform connection topology which is not desirable for a neural network architecture. In this paper, we assign the same r and d for any two cells within the same layer k and index them as $r_{k,l}$ and $d_{k,l}$. We use $r_{k,k}$ and $d_{k,k}$ to denote connections within the same layer (intra-level connections), and $r_{k,l}$ and $d_{k,l}$ with $k \neq l$ for connections between two different layers (extra-level connections). Three different kinds of intra-level connections for a 2-dimensional generalized CNN are shown in Figure 3. Here, the cell located at the center is connected to the cells belonging to its nearest neighborhood determined by r and d. In Figure 3a, the metric is defined by $d_{k,k}(i_1,i_2,k;\hat{i}_1,\hat{i}_2,k) = |i_1 - \hat{i}_1| + |i_2 - \hat{i}_2|$, consequently, its nearest neighborhood consists of only 4 neighbor cells. In Figure 3b, the metric is defined by $d_{k,k}(i_1,i_2,k;\hat{i}_1,\hat{i}_2,k) = \max\{|i_1 - \hat{i}_1|, |i_2 - \hat{i}_2|\}$, and the nearest neighborhood in this case consists of all 8 neighbor cells. Finally, in Figure 3c, the metric is defined by $d_{k,k}(i_1,i_2,k;\hat{i}_1,\hat{i}_2,k) = |i_1 - \hat{i}_1| + |i_2 - \hat{i}_2|$, and the nearest neighborhood in this case consists of 12 neighbor cells.

Figure 3

As in the generalized CNN of Figure 1, and in the Multi-layer Perceptron [5], any two successive layers in a neural network may be fully-connected. However, we can create many different extra-level connection topologies based on the choice of r and d. Two special examples are shown in Figure 4. For both examples, the cell at the center of the lower layer is connected to the 1-nearest neighbors in the upper layer but with two different kinds of neigborhood defined by different metrics: the metric in Figure 4a is defined by $d_{k,k+1}(i,k;\hat{i},k+1) = |i_1 - \hat{i}_1| + 1$, whereas that in Figure 4b is defined by $d_{k,k+1}(i,k;\hat{i},k+1) = \max\{|i_1 - \hat{i}_1|, 1\}$.

Figure 4

Circuit Structure of a Cell :

The connection topology of a generalized CNN has been described above. Now, we present a circuit structure for a cell. Each cell C_i is, in general, an t_i th order nonlinear dynamical circuit such that the circuit topology, elements and/or element values may differ from one cell to another. The cells, considered in this paper, consists of three basic units as shown in Figure 5.

Figure 5

The first unit, which is a multi-input, single-output, linear, resistive circuit, forms a weighted sum of external inputs and the outputs of the neighbor cells. The output of the first unit, e_i , is fed into the second unit. The second unit is a single-input (e_i), single-output (ξ_i), t_i–order linear dynamical circuit. The only nonlinear part of the cell is the third unit which receives ξ_i and pass it through a nonlinearity $f_i(\bullet)$. Such a cell is described by the following system of equations:

$$\dot{x}_i(t) = A_i \cdot x_i(t) + b_i \cdot e_i(t) \tag{1}$$

$$\xi_i(t) = c_i^T \cdot x_i(t) + h_i \cdot e_i(t) \tag{2}$$

$$y_i(t) = f_i(\xi_i(t)) \tag{3}$$

$$e_i(t) = \sum_{\hat{i} \in Y} w_{i,\hat{i}} \cdot y_{\hat{i}}(t - \tau_{i,\hat{i}}) + \sum_{\hat{i} \in Y} z_{i,\hat{i}} \cdot u_{\hat{i}}(t - \sigma_{i,\hat{i}}) + I_i \tag{4}$$

where $A_i \in R^{t_i \times t_i}$; b_i , $c_i \in R^{t_i}$; h_i , $w_{i,\hat{i}}$, $z_{i,\hat{i}}$, $\tau_{i,\hat{i}}$, $\sigma_{i,\hat{i}}$, $I_i \in R$ are all constants; $x_i(\bullet) : R \to R^{t_i}$; $e_i(\bullet)$, $x_i(\bullet)$ and $y_i(\bullet) : R \to R$ are functions of time t; $\dot{x}_i = \frac{dx_i}{dt}$; $f_i(\bullet) : R \to R$ is a nonlinear function; $Y = \{ p | C_p \in B_i \}$ is the set of integers indexing the neighbor cells; here $p = (p_1, p_2, \ldots, p_n, s)$; and $i = (i_1, i_2, \ldots, i_n, k)$, $\hat{i} = (\hat{i}_1, \hat{i}_2, \ldots, \hat{i}_n, l)$ with p_j , i_j , $\hat{i}_j \in \{ 1, 2, \ldots, N_j \}$ for all $j \in \{ 1, 2, \ldots, n \}$ and s , k , $l \in \{ 1, 2, \ldots, m \}$. Each cell has two different kinds of external inputs: $u_i(t)$ and I_i . The controlling input u_i associated with the cell C_i is also applied through the weights $z_{i,\hat{i}}$ to the neighbor cells while the constant input I_i is fed

only into the cell C_1. The delay times $\tau_{1,j}$ and $\sigma_{1,j}$ in (4) are introduced here to obtain a more realistic model. $\tau_{1,j}$ and, respectively, $\sigma_{1,j}$ reflects the propagation time needed for a cell, C_1, to receive the feedback signals $y_j(t)$ and, respectively, the controlling input signals $u_j(t)$ from the neighbor cells. The coefficients $w_{1,j}$ and $z_{1,j}$ in (4) weights the delayed signals $y_j(t-\tau_{1,j})$ and $u_j(t-\sigma_{1,j})$, respectively. For more generality, we can allow $y_j(t)$, $y_j(t - \tau_{1,j}^1)$, $y_j(t - \tau_{1,j}^2)$,..., $y_j(t - \tau_{1,j}^k)$ as well as $u_j(t)$, $u_j(t - \sigma_{1,j}^1)$, $u_j(t - \sigma_{1,j}^2)$,..., $u_j(t - \sigma_{1,j}^k)$ as inputs to Unit I in Figure 5. However, such a model can be transformed into the model described by the equations in (1)-(4) by adding virtual cells.

Special Case I : Cellular Neural Networks

The generalized CNN given by (1)-(4) is a generalization of CNN introduced in [1]. A one layer CNN is obtained as a special case of generalized CNN when the following assumptions are made:

(A1) : The network is a 2-dimensional array of cells;

(A2) : The linear dynamical subcircuit of each cell is of order 1 ($t_1 = 1$);

(A3) : All delay times are zero ($\tau_{1,j} = \sigma_{1,j} = 0$) ;

(A4) : The nonlinear function is the same for all cells and is a continuous piecewise-linear function defined by

$$f(\xi_i) = \frac{1}{2} \{ |\xi_i + 1| - |\xi_i - 1| \} \tag{5}$$

here $|\bullet|$ denotes the absolute value function given by $|\xi_i| = \xi_i$ for $\xi_i > 0$, $= -\xi_i$ for $\xi_i < 0$, and $= 0$ for $\xi_i = 0$;

(A5) : $b_1 = c_1 = 1$, $h_1 = 0$ and A_1 is a negative scalar;

(A6) : $A_1 = -A < 0$ and, respectively, $I_1 = I$ is the same for all cells; and

(A7) : Each cell is connected to the cells in its nearest neighborhood defined by the following metric:

$$d(i_1,i_2;\hat{i}_1,\hat{i}_2) = \max \{ |i_1 - \hat{i}_1|, i_2 - \hat{i}_2| \} . \tag{6}$$

Under the above assumptions (A1)-(A7), the system of equations in (1)-(4) can be rewritten as follows:

$$\dot{x}_{i_1,i_2}(t) = -A \cdot x_{i_1,i_2}(t) + \sum_{\hat{i}_1,\hat{i}_2 \in Y} w_{i_1,i_2;\hat{i}_1,\hat{i}_2} \cdot y_{\hat{i}_1,\hat{i}_2}(t) + \sum_{\hat{i}_1,\hat{i}_2 \in Y} z_{i_1,i_2;\hat{i}_1,\hat{i}_2} \cdot u_{\hat{i}_1,\hat{i}_2}(t) + I \qquad (7)$$

$$y_{i_1,i_2}(t) = \frac{1}{2} \{ |x_{i_1,i_2}(t)+1| - |x_{i_1,i_2}(t)-1| \} . \qquad (8)$$

Special Case II : Hopfield Network

CNN is not the only important subclass of generalized CNN given by (1)-(4). generalized CNN covers quite a large class of neural networks including many well-known neural network architectures such as HN [4] and MP [5]. HN is a 2-dimensional, single-layer generalized CNN where each cell is connected to every other cell. If we assume (A8)-(A10) given below, in addition to the (A1)-(A3) and (A6), the generalized CNN in (1)-(4) reduces into the HN. The additional assumptions are:

(A8) : Each nonlinearity is a sigmoidal function, i.e., $f_i(\bullet) = sgm_i(\bullet) : R \rightarrow (-1,1)$ is continuously differentiable, strictly increasing (i.e., $\dfrac{df_i(\xi_i)}{d\xi_i} > 0$), $\xi_i \cdot f_i(\xi_i) > 0$ for all $\xi_i \neq 0$, and $f_i(0) = 0$;

(A9) : $w_{i,i} = 0$ and $u_i(t) = 0$ for all i ;

(A10) : The network is fully connected. This means the neighborhood of any cell contains all cells in the network. Such a neighborhood can be obtained by choosing $r = 1$ and $d(i_1,i_2;\hat{i}_1,\hat{i}_2) = 0$.

The system of equations defining HN can be written, as in (9)-(10), by using a single index i for each cell. $i = i_1 + N_1 \cdot i_2$ denotes a possible transformation from the double index (i_1,i_2) to i . The resulting system of equations are given as follows:

$$\dot{x}_i(t) = A_i \cdot x_i(t) + \sum_{for\,all\,\hat{i}} w_{i,\hat{i}} \cdot y_{\hat{i}}(t) + I_i \qquad (9)$$

$$y_i(x_i(t)) = sgm_i(x_i(t)) \qquad (10)$$

Special Case III : Multi-layer Perceptron

The MP can also be obtained as a special case of generalized CNN if we assume (A11)-(A16) together with (A3). The additional assumptions are :

(A11) : The network has m layers (typically m 3) each of which is a 1-dimensional array of cells;

(A12) : The cells do not contain a dynamical part, i.e., $t_1 = 0$;

(A13) : $\xi_l(t) = e_l(t)$, i.e., $h_1 = 1$;

(A14) : The nonlinearity is a signum function defined as $f_1(\xi_l) = sgn(\xi_l) = 1$ for $\xi_l > 0$, $= -1$ for $\xi_l < 0$, and $= 0$ for $\xi_l = 0$;

(A15) : There is no intra-level connection. This connection topology can be obtained by choosing a suitable metric such as $d_{k,k}(i,\hat{i}) = 1$, and assuming $r_{k,k} = 0$.

(A16) : Every two successive layers are fully interconnected, i.e., each cell in a layer is connected to every cell in the next layer.

With these assumptions, our generalized CNN reduces to an MP, which can be characterized by the following nonlinear algebraic equations :

$$y_{i,k}(t) = sgn(\xi_{i,k}(t)) \tag{11}$$

$$\xi_{i,k}(t) = e_{i,k}(t) \tag{12}$$

$$e_{i,1}(t) = \sum_{for\,all\,i} z_{i,1;i,1} \cdot u_{i,1}(t) + I_{i,1} \tag{13}$$

$$e_{i,k}(t) = \sum_{for\,all\,i} w_{i,k;i,k-1} \cdot y_{i,k-1}(t) + I_{i,k} \qquad for\,all\; k \in \{\,2,3,...,m\,\} \; . \tag{14}$$

Here, the subscript (i,k) corresponds to the i th cell in the k th layer.

As can be seen from (13)-(14), each cell in the first layer is fed by the external inputs only and the cells in another layer are fed by only the outputs of the cells in the previous layer. Each cell forms a weighted sum of its inputs, adds a threshold $I_{i,k}$ and passes the result through the nonlinearity such that the output is either $+1$ or -1 except for zero total input (i.e., $e_{i,k} = 0$).

Special Case IV : Space-invariant generalized CNN

An important subclass of CNN can be characterized simply by a CNN cloning template [1]. As shown in [1] this subclass is especially useful for image processing applications. A space-invariant

generalized CNN can also be characterized by a generalized CNN cloning template where the space-invariant property is defined as follows.

Definition 2 : A layer of a generalized CNN, say the k th layer, has the space invariant property if each cell $C_{i_1,i_2,\ldots,i_n,k}$ in the k th layer has the same interconnection pattern, i.e., the nearest neigborhood of each cell, $B_{i,k}$, is defined by the same $r_{k,k}$ and the same metric $d_{k,k}$, and the connection weights $w_{i,i}$ and $z_{i,i}$ are invariant under a coordinate transformation; namely,

$$w_{i,\hat{i}} = w_{i-q,\hat{i}-q} \quad ; \quad z_{i,\hat{i}} = z_{i-q,\hat{i}-q} \qquad \text{for } all \text{ q}$$

where, $i = (i_1,i_2,\ldots,i_n,k)$, $\hat{i} = (\hat{i}_1,\hat{i}_2,\ldots,\hat{i}_n,k)$ and $q = (q_1,q_2,\ldots,q_n,0)$ with i_j , $\hat{i}_j$ and $q_j \in \{1,2,\ldots,N_j\}$ for all $j \in \{1,2,\ldots,n\}$.

If all layers of a generalized CNN have the space invariant property, then the generalized CNN is said to be space invariant. □

Note that the cells on the boundaries of the layers always fail the condition in Definition 2 and they should be considered separately. However, one can obtain a uniform structure by adding virtual cells beyond the boundaries [13].

Observe that, for a space invariant generalized CNN, a set of coefficients specifying the connection weights associated with any non-boundary cell is sufficient to express all other coefficients. Consequently, it is convenient to express the coefficients of $w_{i,\hat{i}}$ and $z_{i,\hat{i}}$ as the elements of the sets W_k and Z_k defined as:

$$W_k(i-\hat{i}) = w_{i,\hat{i}}$$
$$Z_k(i-\hat{i}) = z_{i,\hat{i}}$$

where, the center elements $W_k(0,0,\ldots,0)$ (respectively, $Z_k(0,0,\ldots,0)$) denote the coefficients which weights the self output (respectively, self input) of any cell in the k th layer. Similarly, all other elements $W_k(i-\hat{i})$ and $Z_k(i-\hat{i})$ do not depend on i ; they depend only on k (indexing the layers) and on $i-\hat{i}$, which represents the relative position of the neighbor cell $C_{\hat{i}}$ with respect to the center cell C_i . Observed that the number of elements in the set W_k or Z_k is equal to the number of cells in the nearest neigborhood $B_{i,k}$. For a 2-dimensional generalized CNN, the coefficents $W_k(i-\hat{i})$ and

$Z_k(i-\hat{i})$ can be considered as elements of the matrices $\mathbf{W}_k$ and $\mathbf{Z}_k$, respectively, where, $W_k(i,j)$ and $Z_k(i,j)$ denotes the entry in the i th row and the j th column of the matrix $\mathbf{W}_k$ and $\mathbf{Z}_k$, respectively.

III. STABILITY OF ISOLATED CELLS

The aim of this section is twofold: i) to show by some concrete examples that the cells of generalized CNN have a rather rich repertoire of nonlinear dynamic behaviors, including oscillation and chaos; and their capabilities, as proccesing elements, go well beyond the ones provided by the common 0 th order cells (as in Perceptron) and 1 st order cells (as in CNN and Hopfield net); and ii) to give a set of conditions ensuring the input-output stability, and/or global asymptotic stability, of the isolated cells.

It will become transparent in this section that the neural network model proposed in this paper covers quite a large class of neural networks and, with its capabilities, it offers a promising architecture for biological nervous systems as well as for electronic neural networks.

It is shown below that the problem of finding the conditions ensuring the global asymptotic stability for an isolated cell with zero input is in fact the well-known Lur'e problem for which many comprehensive results are available in the literature [7]-[9]. Our results on generalized CNN input-output stability are based on Lemmas 1 and 2. For the developement of Lemmas 1 and 2, and the earlier works on the input-output stability, see [8].

Let us describe what we mean by isolated cells. An isolated cell $C_{\hat{i}}$ is obtained by setting all connection weights between $C_{\hat{i}}$ and its neighbors to zero, i.e., $w_{\hat{i},i} = z_{\hat{i},i} = 0$ for all $i \neq \hat{i}$. Such an isolated cell is described by the following equations.

$$\dot{\mathbf{x}}_{\hat{i}}(t) = \mathbf{A}_{\hat{i}} \cdot \mathbf{x}_{\hat{i}}(t) + \mathbf{b}_{\hat{i}} \cdot e_{\hat{i}}(t) \tag{15}$$

$$\xi_{\hat{i}}(t) = \mathbf{c}_{\hat{i}}^T \cdot \mathbf{x}_{\hat{i}}(t) + h_{\hat{i}} \cdot e_{\hat{i}}(t) \tag{16}$$

$$y_{\hat{i}}(t) = f_{\hat{i}}(\xi_{\hat{i}}(t)) \tag{17}$$

$$e_i(t) = w_{i,i} \cdot y_i(t - \tau_{i,i}) + z_{i,j} \cdot u_i(t - \sigma_{i,j}) + I_i \tag{18}$$

As illustrated in Figure 6, each isolated cell can be considered as a feedback system whose forward path contains a t_i th order linear time-invariant dynamical subsystem and whose feedback path contains a memoryless nonlinearity and a delay line.

Figure 6

Therefore, the stability analysis of isolated cells amounts to seeking the conditions which ensure the stability of such a nonlinear feedback system. A large amount of reults [7]-[9] is available for this feedback system. The following Theorems 1 and 2 are two applications of these results for neural networks.

In contrast with the models given in the literature [1],[3]-[5], we do not make any assumption on the nonlinearity $f_i(\bullet)$ in our generalized CNN model. This allows us to present our results in as general a context as possible, and also to see how the choice of the nonlinearity affects the dynamic behaviors of the generalized CNN.

Let us first demonstrate that an isolated cell possessing chaotic dynamics can be constructed by choosing an appropriate nonlinearity $f_i(\bullet)$.

Example 1 : Chua's Circuit

Consider a 3 rd order cell defined by

$$\dot{x}_i(t) = \begin{bmatrix} -\dfrac{G}{C_1} & \dfrac{G}{C_1} & 0 \\ \dfrac{G}{C_2} & -\dfrac{G}{C_2} & \dfrac{1}{C_2} \\ 0 & -\dfrac{1}{L} & 0 \end{bmatrix} \cdot x_i(t) + \begin{bmatrix} -\dfrac{1}{C_1} \\ 0 \\ 0 \end{bmatrix} \cdot e_i(t) \tag{19}$$

$$\xi_i(t) = \begin{bmatrix} 1 & 0 & 0 \end{bmatrix} \cdot x_i(t) \tag{20}$$

$$y_i(t) = f_i(\xi_i(t)) = m_0 \cdot \xi_i(t) + \frac{1}{2} \cdot (m_1 - m_0)(|\xi_i(t) + 1| - |\xi_i(t) - 1|) \tag{21}$$

$$e_i(t) = y_i(t) \ , \tag{22}$$

where G, C_1, C_2, L, $-m_0$ and $-m_1$ are positive real numbers. Eliminating the variables e_i, ξ_i and y_i from (19)-(22), we obtain the same set of three piecewise-linear ordinary differential equations which describes the Chua circuit [16] shown in Figure 7a.

Figure 7

This circuit has been investigated in depth; and it has been observed and proved that Chua's circuit possesses rather complicated nonlinear dynamics, including chaotic phenomena [16]. □

As seen in Example 1, even if the linear dynamical subcircuit of a cell consists of some innocent linear passive circuit elements, the nonlinearity in the feedback path may cause very complicated non-linear dynamics. In the stability analysis treated below, we usually assume the nonlinearity $f_i(\bullet)$ satisfies the sector conditions given in Definition 3.

Definition 3 : Let $f_i(0) = 0$. We say the function $f_i(\bullet)$ belongs to the sector (k_1, k_2) if $k_1 \cdot \xi_i^2 < \xi_i \cdot f_i(\xi_i) < k_2 \cdot \xi_i^2$ for all $\xi_i \neq 0$. Similarly, $f_i(\bullet)$ belongs to the sector $[k_1, k_2)$ if $k_1 \cdot \xi_i^2 \leq \xi_i \cdot f_i(\xi_i) < k_2 \cdot \xi_i^2$ for all $\xi_i \neq 0$. □

As illustrated in Figure 8, a continuous function $f_i(\bullet)$ belongs to the open sector (k_1, k_2) if the graph of $f_i(\xi_i)$ versus ξ_i lies between and does not touch the straight lines passing through the origin with slopes k_1 and k_2 , respectively. In the case the graph touches both straight lines, we say $f_i(\bullet)$ belongs to the closed sector $[k_1, k_2]$.

Figure 8

Observed that the nonlinearity used in the CNN (see (5)) belongs to the closed sector $[0, 1]$ while the sigmoid function, defined by

$$f_i(\xi_i) = \frac{2}{\pi} \cdot V \cdot arctan \left(\frac{\pi}{2} \cdot \frac{K}{V} \cdot \xi_i \right) \tag{23}$$

with positive numbers V and K , belongs to the open sector $(0,K)$.

In the sequel, we are concerned not with the stability of a generalized CNN having a particular non-linearity, but with the stability of any generalized CNN having a nonlinearity satisfying some sector conditions. In the literature, such an analysis is referred to as absolute stability analysis.

Input-Output Stability :

In most of the current dynamic neural network applications, the external inputs $u_i(t)$'s are fixed at some constant values, usually zero; and the input data is fed into the network via initial conditions rather than the external inputs. In a CNN or a HN designed in this way, if the interconnection weights are symmetric then every trajectory approaches an equilibrium point that depends on the initial state. Such networks are considered as content-addressable memories where the equilibria are the stored memories, or as classifiers for input patterns. However, the initial conditions of these networks are required to be reset to zero each time the network is run. This is not a desirable property for a network running in real time. It is, therefore, of interest [2] to design a neural network which is fed via external-inputs, possibly time-varying, and then run without resetting the initial conditions.

With the above motivation, we will study the stability of a generalized CNN having time-varying external inputs. Before stating the criteria for the input-output stability of an isolated cell, let us present some basic definitions of input-output stability.

Consider the feedback system shown in Figure 9. Here, the vectors $U_1(t)$, $U_2(t)$ denote the inputs; $Y_1(t)$, $Y_2(t)$ denote the outputs; and $E_1(t)$, $E_2(t)$ denote the errors. The subsystem G_1 and the subsystem G_2 are, in general, nonlinear dynamical systems; and can be defined by an operator which acts on the input $E_1(t)$ and $E_2(t)$, respectively.

Figure 9

For a given $p \in [1,\infty)$, let L_p denote the set of all (Lebesgue) measurable functions $g(\bullet) : [0,\infty) \to \mathbf{R}$ such that

$$\int_0^\infty |g(t)|^p \cdot dt < \infty .$$

Similarly, let L_∞ denote the set of all measurable functions $g(\bullet) : [0, \infty) \to R$ such that

$$\underset{t \in [0,\infty)}{ess.\,sup.} |g(t)| = \inf \{ a : |g(t)| \le a \quad almost \; everywhere \} < \infty$$

i.e., $|g(t)| \le a$ except for a set of measure zero, and the ess.sup. (essential supremum) is the smallest number having that property. The set L_{pe}, called the extended L_p-space, is the set of all measurable functions $g(\bullet) : [0, \infty) \to R$ having the property that for all $T \in [0, \infty)$ the truncation $g_T(\bullet)$ of $g(\bullet)$ belongs to L_p; where $g_T(\bullet)$ is defined by

$$g_T(t) = g(t) \quad if \; 0 \le t \le T ,$$
$$= 0 \quad if \; T < t .$$

The symbol L_p^q denotes the set of all q-tuples $g(\bullet) = [g_1(\bullet) \cdots g_q(\bullet)]^T$, where $g_i(\bullet) \in L_p$ for all $i \in \{ 1,2,...,q \}$. L_{pe}^q is defined similarly. The norm on L_p^q is given by

$$\|g(\bullet)\|_p = [\sum_{i=1}^q \|g_i(\bullet)\|_p^2]^{\frac{1}{2}}$$

with $\|g_i(\bullet)\|_p = [\int_0^\infty |g_i(t)|^p \cdot dt]^{\frac{1}{p}}$ for $p \in [1, \infty)$ and $\|g_i(\bullet)\|_\infty = \underset{t \in [0,\infty)}{ess.\,sup.} |g_i(t)|$.

Definition 4 : The system, shown in Figure 9, is said to be L_p-stable provided that, for any inputs $U_1(\bullet)$, $U_2(\bullet) \in L_p^q$, if we have outputs $Y_1(\bullet)$, $Y_2(\bullet) \in L_{pe}^q$ then $Y_1(\bullet)$, $Y_2(\bullet) \in L_p^q$; and, in addition, there exist finite constants r_1 and r_2 such that

$$\|Y_1(\bullet)\|_p \le r_1 \cdot (\|U_1(\bullet)\|_p + \|U_2(\bullet)\|_p) + r_2 \tag{24}$$

$$\|Y_2(\bullet)\|_p \le r_1 \cdot (\|U_1(\bullet)\|_p + \|U_2(\bullet)\|_p) + r_2 . \quad \Box \tag{25}$$

One important special case of L_p-stability is the L_∞-stability which is commonly referred to as BIBO (bounded-input/bounded output) stability. Observe that BIBO stability means bounded inputs produce bounded outputs and (24)-(25) hold.

Now, we present the circle criterion which provides a sufficient condition for L_2-stability for the

feedback system shown in Figure 9, but with scalar inputs $U_1(t)$, $U_2(t) \in \mathbf{R}$ and scalar outputs $Y_1(t)$, $Y_2(t) \in \mathbf{R}$.

Lemma 1 [8] : Circle Criterion

Consider the scalar feedback system shown in Figure 9, where $U_1(t)$, $U_2(t)$, $E_1(t)$, $E_2(t)$, $Y_1(t)$ and $Y_2(t) \in \mathbf{R}$. The subsystem G_1 is linear, time-invariant, possibly distributed and described by the following convolution operator

$$Y_1(t) = G_1(t) * E_1(t) = \int_0^t G_1(t-\lambda) \cdot E_1(\lambda) \cdot d\lambda \tag{26}$$

where, the impulse response $G_1(\bullet)$ of the subsystem G_1 belongs to L_{pe} and has a Laplace transform $\hat{G}_1(s)$ which is, in general, an irrational function. The subsystem G_2 is memoryless and represented by the algebraic relation

$$Y_2(t) = \psi [E_2(t)] \tag{27}$$

where $\psi(\bullet) : \mathbf{R} \to \mathbf{R}$ belongs to the sector $[\alpha, \beta]$. The system described by (25)-(26) is L_2-stable if the pole locations and Nyquist diagram of $\hat{G}_1(s)$ (i.e., the graph of the map $w \to \hat{G}_1(jw)$ with $w \in [0,\infty)$) satisfy one of the following sets of conditions:

i) If $0 < \alpha < \beta < \infty$, there are no restrictions on the location of the poles of $\hat{G}_1(s)$. However, the Nyquist diagram of $\hat{G}_1(s)$ must satisfy the following properties:

a) the Nyquist diagram of $\hat{G}_1(s)$ is bounded away from the disk D (which is a circle in the complex plane centered on the real axis and passing through the points $\frac{-1}{\alpha} + j \cdot 0$ and $\frac{-1}{\beta} + j \cdot 0$); that is

$$|\hat{G}(jw) - \theta| > 0 \quad \text{for } all \quad w \in \mathbf{R} \quad \text{and} \quad \theta \in D .$$

b) the Nyquist diagram encircles the disk D in the counterclockwise direction exactly ν times, where ν is the number of poles of $\hat{G}_1(s)$ with a positive real part.

ii) If $0 = \alpha < \beta < \infty$, then $\hat{G}_1(s)$ must have no poles in the open right complex half-plane, and the Nyquist diagram of $\hat{G}_1(s)$ must remain to the right of the vertical line $s = \frac{-1}{\beta} + j \cdot 0$; i.e.,

$$\text{Re} \{ \hat{G}_1(jw) \} > \frac{-1}{\beta} \quad \text{for } all \quad w \in \mathbf{R} .$$

iii) If $-\infty < \alpha < 0 < \beta < \infty$, $\hat{G}_1(s)$ has no poles in the closed right half-plane, and the Nyquist diagram of $\hat{G}_1(s)$ is completely contained in the interior of the disk D.

iv) If $-\infty < \alpha < \beta \le 0$, replace $\hat{G}_1(s)$ by $-\hat{G}_1(s)$, α by $-\beta$, β by $-\alpha$, and apply i) or ii) above, as appropriate. □

Theorem 1 is a direct application of Lemma 1 to generalized CNN.

Theorem 1 :

Assume the nonlinearity $f_1(\bullet)$ belongs to the sector $[k_1, k_2]$ with k_1, k_2 finite. An isolated cell defined by (15)-(18) (with input $z_{1,i}u_i(t - \sigma_{1,i}) + I_1$, linear part output $\xi_i(t)$, output $y_i(t)$ and transmitted output $w_{1,i}y_i(t - \tau_{1,i})$) is L_2-stable if :

i) for zero feedback $w_{1,i} = 0$;

the rational tranfer function

$$\hat{G}_1(s) = c_i^T \cdot [sI - A_1]^{-1} \cdot b_1 + h_1 \tag{28}$$

is proper (i.e., all elements of $\hat{G}_1(s)$ are bounded at $s = \infty$) and all its poles have negative real parts.

ii) for inhibitory feedback $w_{1,i} < 0$;

$\hat{G}_1(s) \cdot e^{-s\tau_{1,i}}$ satisfies one of the sets of conditions i)-iv) given in Lemma 1, but with $\alpha = -w_{1,i} \cdot k_1$, $\beta = -w_{1,i} \cdot k_2$ and $\hat{G}_1(s) \cdot e^{-s\tau_{1,i}}$ instead of $\hat{G}_1(s)$.

iii) for excitatory feedback $w_{1,i} > 0$;

replace β by α and α by β ; and apply ii) .

Proof :

i) $w_{1,i} = 0$ implies that the transmitted output $w_{1,i} \cdot y_i(t - \tau_{1,i})$ is zero for all time t. Then, the only output, which should be examined, is $y_i(t)$. It follows from well-known result for linear systems [8] that $\xi_i(\bullet)$ belongs to L_2 if $e_i(\bullet) \in L_2$; and $\hat{G}_1(s)$ is proper with all its poles in the open left half-plane. From the assumption that $f_1(\bullet)$ belongs to sector $[k_1, k_2]$, we have

$$k_1 \cdot \xi_i^2 \le \xi_i \cdot f_1(\xi_i) \le k_2 \cdot \xi_i^2 \qquad \text{for } all \quad \xi_i \in \mathbf{R} \quad .$$

Observe that

$$0 \geq (\xi_i \cdot f_i(\xi_i) - k_1 \cdot \xi_i^2) \cdot (\xi_i \cdot f_i(\xi_i) - k_2 \cdot \xi_i^2) = \xi_i^2 \cdot (f_i(\xi_i) - k_1 \cdot \xi_i) \cdot (f_i(\xi_i) - k_2 \cdot \xi_i)$$

which implies

$$0 \geq (f_i(\xi_i) - k_1 \cdot \xi_i) \cdot (f_i(\xi_i) - k_2 \cdot \xi_i) = f_i^2(\xi_i) - (k_2 + k_1) \cdot \xi_i \cdot f_i(\xi_i) + k_1 \cdot k_2 \cdot \xi_i^2$$

$$= (f_i(\xi_i) - \frac{k_2 + k_1}{2} \cdot \xi_i)^2 - (\frac{k_2 - k_1}{2})^2 \cdot \xi_i^2 .$$

The last inequality gives

$$|\frac{k_2 - k_1}{2}| \cdot |\xi_i| \geq |f_i(\xi_i) - \frac{k_2 + k_1}{2} \cdot \xi_i| \geq |f_i(\xi_i)| - |\frac{k_2 + k_1}{2}| \cdot |\xi_i| . \tag{29}$$

Therefore, we have

$$|f_i(\xi_i)| \leq \frac{1}{2} \cdot (|k_2 - k_1| + |k_2 + k_1|) \cdot |\xi_i| . \tag{30}$$

It follows from (30) that $y_i(\bullet)$ belongs to L_2 whenever $e_i(\bullet) \in L_2$ (and then $\xi_i(\bullet) \in L_2$).

ii) Consider the isolated cell shown in Figure 6. Let us replace the delay element $e^{-s \tau_{i,i}}$ with the non-linearity $f_i(\bullet)$, and vice versa. The resulting system can be described by a set of equations which are equivalent to the ones in (15)-(18). Therefore, the proof, which will be given below for this new system, is also valid for the original one. The system obtained is, indeed, a feedback system with the forward path transfer function $\hat{G}_i(s) \cdot e^{-s \tau_{i,i}}$ and the feedback nonlinearity $-w_{i,i} \cdot f_i(\bullet)$. Since $\hat{G}_i(s)$ is a rational function, its inverse Laplace transform $G_i(t)$, and then, the impulse response of the forward path, $G_i(t - \tau_{i,i})$ belongs to L_{pe} . With $w_{i,i}$ negative, $-w_{i,i} \cdot f_i(\bullet)$ belongs to the sector $[\alpha, \beta] = [-w_{i,i} \cdot k_1, -w_{i,i} \cdot k_2]$ whenever $f_i(\bullet)$ belongs to the sector $[k_1, k_2]$. Lemma 1 implies that the system, with inputs $U_1(t) = z_{i,i} u_i(t - \sigma_{i,i}) + I_i$, $U_2(t) = 0$ and outputs $Y_1(t) = \xi_i(t)$, $Y_2(t) = -w_{i,i} \cdot y_i(t - \tau_{i,i})$, is L_2-stable. The proof for the other output $y_i(t)$ follows from (30).

iii) Follows from ii) . $\square$

The result obtained by Theorem 1 is important for the following reasons : i) The conditions can be easily checked by a straightforward Nyquist graphical test, which is applied directly to the transfer function of the linear dynamical subcircuit, ii) As will be seen in Theorem 3, the same conditions, plus a more stringent condition on the nonlinearity, ensure also the global asymptotic stability of an isolated cell with constant input, iii) Theorem 1 is applicable to an arbitrary order isolated cell having a transmission

delay, iv) The stability of the linear dynamical subcircuit is not required and v) The L_2-stability analysis is treated in a way which does not depend on the existence of a state equation form, and the existence and uniqueness of the solutions.

Let us apply Theorem 1 to study the L_2-stability of an isolated cell in a CNN.

Example 2 :

It can be verified by the definition of CNN that, for an isolated cell, the nonlinearity $f_i(\bullet)$ belongs to the closed sector $[\,0\,,1\,]$ and the forward path transfer function can be given by $\hat{G}_i(s) = \dfrac{1}{s+A}$ with A positive. For zero feedback $w_{i,i} = 0$; the L_2-stability follows from the observation that $\dfrac{1}{s+A}$ is proper and its pole $-A$ is negative real. For inhibitory feedback $w_{i,i} < 0$, condition ii) in Lemma 1 should be applied since $\alpha = 0$ and $\beta = -w_{i,i} > 0$. The inequality

$$\text{Re }\{\ \hat{G}_i(jw)\ \} = \text{Re }\{\ \frac{1}{jw+A}\ \} = \frac{A}{A^2+w^2} > \frac{1}{w_{i,i}}$$

holds for all $w \in \mathbf{R}$ if and only if $A < -w_{i,i}$. For excitatory feedback $w_{i,i} > 0$, condition iv) in Lemma 1 is appropriate to be applied since $\alpha = -w_{i,i} < 0$ and $\beta = 0$. Now, we have the inequality

$$\text{Re }\{\ -\hat{G}_i(jw)\ \} = \text{Re }\{\ \frac{-1}{jw+A}\ \} = \frac{-A}{A^2+w^2} > \frac{-1}{w_{i,i}}$$

which holds for all $w \in \mathbf{R}$ if and only if $w_{i,i} < A$. We conclude that an isolated cell of a CNN is L_2-stable if the feedback weight $w_{i,i}$ lies in one of the following intervals : $0 \le w_{i,i} < A$ or $w_{i,i} < -A < 0$. The region of L_2-stability obtained by Theorem 1 is illustrated in Figure 10 where $w_{i,i}$ is the parameter. $\square$

Figure 10

Although Theorem 1 is important for the reasons mentioned above, the input-output stability analysis based on this theorem suffers from the following two drawbacks : i) Theorem 1 provides conditions for only L_2-stability whereas some important source signals, such as sinusoidal or constant signals, do not belong to L_2 , and ii) Since Theorem 1 does not exploit the boundedness of the nonlinearity, it yields

rather conservative results for those neural networks, such as CNN or HN, having a saturation-type non-linearity.

The first drawback is overcome by Theorem 2, to be presented below, which provides a set of sufficient conditions for the L_∞-stability of an isolated cell. The latter will be considered, in the most general case, in section IV, where a theorem using the boundedness of the nonlinearity is presented.

This theorem is based on the following lemma.

Lemma 2 [8] : L_∞-stability

Consider the scalar feedback system shown in Figure 9, where, $U_1(t)$, $U_2(t)$, $E_1(t)$, $E_2(t)$, $Y_1(t)$, $Y_2(t) \in \mathbf{R}$, and $U_2(t) \equiv 0$. The subsystem G_1 is linear, time-invariant, possibly distributed, and described by the convolution operator

$$Y_1(t) = G_1(t) * E_1(t) .$$

Assume the impulse response $G_1(t)$ has a Laplace transform $\hat{G}_1(s)$ and satisfies the following exponential weighting condition:

$$e^{at} \cdot G_1(t) \in L_1 \cap L_2 \quad \text{for } some \quad a > 0 . \tag{31}$$

The system G_2 is memoryless and represented by the following algebraic relation

$$Y_2(t) = \psi [E_2(t)]$$

such that $\psi(\bullet) : \mathbf{R} \to \mathbf{R}$ belongs to the closed sector $[\alpha , \beta]$ with β , α finite. Under these conditions, if the a-shifted Nyquist diagram of $\hat{G}_1(s)$,i.e., the graph of the map $w \to \hat{G}_1(-a + jw)$, satisfies one of the conditions i)-iv) in Lemma 1, then $U_1(\bullet) \in L_\infty$ implies $E_1(\bullet)$, $Y_1(\bullet) \in L_\infty$, and moreover, there exist finite constants $l_1 > 0$ and $l_2 > 0$ such that

$$\| E_1(\bullet) \|_\infty \le l_1 \cdot \| U_1(\bullet) \|_\infty \tag{32}$$

$$\| Y_1(\bullet) \|_\infty \le l_2 \cdot \| U_1(\bullet) \|_\infty . \quad \Box \tag{33}$$

Our next theorem is a direct application of Lemma 2 to neural networks.

Theorem 2 :

Consider an isolated cell described by (15)-(18). Assume that i) the nonlinearity $f_1(\bullet)$ belongs to the closed sector $[k_1 , k_2]$ with k_2 , k_1 finite, and ii) $\hat{G}_1(s)$, defined in (28), is strictly proper

(i.e., all elements of $\hat{G}_1(s)$ tend to zero at $s = \infty$) and all of its poles p_j have negative real parts. Under these conditions; for some $a \geq -\operatorname{Re} p_j > 0$ if the a-shifted Nyquist diagram of $\hat{G}_1(s) \cdot e^{-s \tau_{1,i}}$ satisfies the conditions i)-iii) in Theorem 1, then $u_1(\bullet)$ belongs to L_∞ implies $\xi_1(\bullet) \in L_\infty$, $y_1(\bullet) \in L_\infty$, $w_{1,i} \cdot y_1(\bullet - \tau_{1,i}) \in L_\infty$, and moreover, there exists a finite constant $l > 0$ such that

$$\| \xi_1(\bullet) \|_\infty \leq l \cdot |z_{1,i}| \cdot \| u_1(\bullet) \|_\infty + l \cdot |I_1| \tag{34}$$

$$\| y_1(\bullet) \|_\infty \leq l \cdot k \cdot |z_{1,i}| \cdot \| u_1(\bullet) \|_\infty + l \cdot k \cdot |I_1| \tag{35}$$

$$\| w_{1,i} \cdot y_1(\bullet - \tau_{1,i}) \|_\infty \leq l \cdot k \cdot |z_{1,i}| \cdot |w_{1,i}| \cdot \| u_1(\bullet) \|_\infty + l \cdot k \cdot |w_{1,i}| \cdot |I_i| \tag{36}$$

where, $k = \frac{1}{2} \cdot (|k_2 - k_1| + |k_2 + k_1|)$.

Proof:

As in the Theorem 1, the proof will be done in three steps corresponding to three different values of $w_{1,i}$; namely, zero, negative and positive. First, observe that the total input $z_{1,i} \cdot u_1(\bullet - \sigma_{1,i}) + I_1$ belongs to L_∞ whenever $u_1(\bullet) \in L_\infty$ since I_1 is constant. Moreover,

$$\| z_{1,i} \cdot u_1(\bullet - \sigma_{1,i}) + I_1 \|_\infty \leq |z_{1,i}| \cdot \| u_1(\bullet) \|_\infty + |I_1| \ . \tag{37}$$

i) Zero feedback case:

$\xi_1(\bullet) \in L_\infty$ if $u_1(\bullet)$ belongs to L_∞ since $\hat{G}_1(s)$ is strictly proper and all of its poles are in the open left half-plane [8]. The bound (34) follows from (37) and the L_∞-stability of the linear forward path. The bound (35) is obtained by using the result in (30) and (34).

ii)-iii) Negative and positive feedback cases:

When $\hat{G}_1(s)$ is strictly proper with all of its poles in the open left half-plane, the exponential weighting condition

$$e^{at} \cdot G_1(t) \in L_1 \cap L_2$$

is satisfied for any positive real a with $a < -\operatorname{Re} \{ p_j \}$ for all poles p_j of $\hat{G}_1(s)$. The $\tau_{1,i}$-

shifted impulse response $G_i(t - \tau_{i,j})$ also satisfies the exponential weighting condition with the same a . This fact, together with Lemma 2, implies that $\xi_i(\bullet) \in L_\infty$ if $u_i(\bullet) \in L_\infty$. Hence, (34)-(36) follows from (33), (37) and (30). $\square$

Our next example asserts that, for an isolated cell of a CNN, L_∞-stability is ensured by a set of conditions similar to those for L_2-stability.

Example 3 :

Consider an isolated cell of a CNN. We can show that the results given in Example 2 are also valid for L_∞-stability but with A replaced by $A - a$. The region of L_∞-stability is obtained as the union of ' the intervals : $0 \le w_{i,i} < A - a$ and $w_{i,i} < -A + a < 0$ where a is an arbitrary small positive number less than A . $\square$

Global Asymptotic Stability :

In the sequel, a set of conditions for the global asymptotic stability of an isolated cell is given. The results are useful for the design of a neural network having a unique globally asymptotic stable equilibrium point which depends on the input.

As known in the literature [9], the conditions ensuring the input-output stability of the system considered in Lemma 1, are also sufficient conditions for the global asymptotic stability of the system with zero-input. We shall show by Theorem 3 that, under the conditions given for L_2-stability, an isolated cell is globally asymptotically stable for each constant input if the sector condition is replaced by the following more stringent condition, henceforth called the incremental sector condition.

Definition 5 : An $f_i(\bullet)$, with $f_i(0) = 0$, satisfies the incremental sector condition if there exist real constants k_1 and k_2 satisfying $k_2 \ge k_1$ such that

$$k_1 \cdot (\xi_i' - \xi_i'')^2 \le (\xi_i' - \xi_i'') \cdot (f_i(\xi_i') - f_i(\xi_i'')) \le k_2 \cdot (\xi_i' - \xi_i'')^2 \quad \text{for all } \xi_i' , \xi_i'' \in R . \square \qquad (38)$$

Condition (38) gives a sector condition with $\xi_i' = \xi_i$ and $\xi_i'' = 0$. A function $f_i(\bullet)$, which satisfies (38), is monotonically increasing, uniformly increasing, and strongly-uniformly increasing if $\infty \ge k_2 \ge k_1 = 0$, $\infty \ge k_2 \ge k_1 > 0$ and $\infty > k_2 \ge k_1 > 0$, respectively. A function $f_i(\bullet)$, satisfying the incremental sector condition with finite k_1 , k_2 is Lipschitz continuous with the Lipschitz

constant $\frac{1}{2} \cdot (|k_2 - k_1| + |k_2 + k_1|)$:

$$|f_i(\xi_i') - f_i(\xi_i'')| \leq \frac{1}{2} \cdot (|k_2 - k_1| + |k_2 + k_1|) \cdot |\xi_i' - \xi_i''| \tag{39}$$

One can verify (39) by the same algebraic manipulations used in the derivation of (30). On the other hand, if $f_i(\bullet)$ is differentiable, then its derivative satisfies the following inequalities :

$$k_1 \leq \frac{df_i(\xi_i)}{d\xi_i} \leq k_2 . \tag{40}$$

For the rest of this section, it is assumed that $f_i(\bullet)$ satisfies the incremental sector condition, and the input $u_i(t)$ is a constant and denoted by U_i .

We shall now present the definitions of complete stability and global asymptotic stability for a system defined by the autonomous differential equations

$$\dot{x}(t) = F[x(t)] \tag{41}$$

where $x(t)$ is a vector.

Definition 6 : A system decribed by the equations in (41) is said to be completely stable if each solution $x(t)$ converges to an equilibrium point as $t \rightarrow \infty$. $\square$

Definition 7 : The system is said to be globally asymptotically stable if each solution $x(t)$ converges to a unique equilibrium point. $\square$

The equations in (15)-(18) which describe an isolated cell are, in general, not in the state equation form. Therefore, the stability definitions given above can not be applied directly to generalized CNN. However, if $\tau_{i,j} = 0$ and the nonlinear algebraic relation

$$\xi_i(t) = c_i^T \cdot x_i(t) + h_i \cdot w_{i,j} \cdot f_i(\xi_i(t)) + h_i \cdot z_{i,j} \cdot U_i + h_i \cdot I_i \tag{42}$$

can be solved for $\xi_i(t)$ in terms of the state vector x_i and the inputs, then the equations in (15)-(18) can be rewritten in a state equation form. The local solvability of the relation (42) is in fact not an extra assumption for the absolute (global asymptotic) stability of a cell because, i) it is a necessary precondition for the absolute stability that the cell governed by the equations (15)-(18) must be globally asymptotically stable for all linear feedbacks $f_i(\xi_i) = K \cdot \xi_i$ with $K \in [k_1, k_2]$; ii) this precondition requires

$$1 \neq K \cdot w_{i,i} \cdot h_i \tag{43}$$

Indeed, if (43) is not satisfied, then the closed loop transfer function

$$\frac{\hat{G}_i(s)}{1 - K \cdot w_{i,i} \cdot \hat{G}_i(s)}$$

is not proper and so represents an unstable system [8]. **iii)** It follows from the well-known local implicit function theorem that the relation (42), with a locally differentiable nonlinearity $f_i(\bullet)$ satisfying (38), is locally solvable for ξ_i since the condition (43) together with (40) implies the slope of $\xi_i - w_{i,i} \cdot h_i \cdot f_i(\xi_i)$ is nonzero at each point. By the above facts, we can always assume a locally defined state equation exists in a neigborhood of some specific point, such as an equilibrium point, for cells without time delays, assuming the nonlinearity is differentiable.

On the other hand, for $\tau_{i,i} \neq 0$, the equations in (15)-(18) constitute a set of algebraic and differential difference equations. Eliminating the variables $y_i(t)$ and $e_i(t)$, these equations can be recast into the form:

$$\dot{x}_i(t) = A_i \cdot x_i(t) + b_i \cdot w_{i,i} \cdot f_i(\xi_i(t - \tau_{i,i})) + b_i \cdot z_{i,i} \cdot U_i + b_i \cdot I_i \tag{44}$$

$$\xi_i(t) = c_i^T \cdot x_i(t) + h_i \cdot w_{i,i} \cdot f_i(\xi_i(t - \tau_{i,i})) + h_i \cdot z_{i,i} \cdot U_i + h_i \cdot I_i . \tag{45}$$

Observe that we can consider $\xi_i(t)$ also as a state variable in addition to the state vector $x_i(t)$. However, in order to find a solution to the equations (44)-(45), we need to know the initial state vector $x_i(0)$ and the initial function $\xi_i(t) = \theta_i(t)$ with $t \in [-\tau_{i,i}, 0]$ [20]. The initial function $\theta_i(\bullet)$ which is defined in the interval $[-\tau_{i,i}, 0]$, is assumed to belong to L_2 . An equilibrium point $((x_i^*)^T, \xi_i^*)^T$ of the differential-difference equations (44)-(45) is defined as a solution to the following algebraic equations.

$$0 = A_i \cdot x_i^* + b_i \cdot w_{i,i} \cdot f_i(\xi_i^*) + b_i \cdot z_{i,i} \cdot U_i + b_i \cdot I_i \tag{46}$$

$$\xi_i^* = c_i^T \cdot x_i^* + h_i \cdot w_{i,i} \cdot f_i(\xi_i^*) + h_i \cdot z_{i,i} \cdot U_i + h_i \cdot I_i . \tag{47}$$

With the above generalization of state variables, initial conditions, and equilibrium points, our definitions 6 and 7 on complete stability and global asymptotic stability for ordinary differential equations can also be adopted for the differential-difference equations (44)-(45).

Throughout our complete and global asymptotic stability analysis, we shall assume that (44)-(45), and respectively (41), has a unique solution over $[\,0\,,\infty\,]$ corresponding to each initial condition. A sufficient condition ensuring the existence and uniqueness of the solutions for a generalized CNN is given in section IV.

As mentioned above, the absolute (global asymptotic) stability requires the local solvability of (47) with respect to ξ_i^*, i.e., the existence of a locally defined function

$$\xi_i^* = \xi_i^*(x_i^*, U_i, I_i) \tag{48}$$

which expresses ξ_i^* in terms of the x_i^* and the inputs. Similarly, observe that if an isolated cell is absolutely stable, then the system of algebraic equations

$$0 = A_i \cdot x_i^* + b_i \cdot w_{i,i} \cdot f_i(\xi_i^*(x_i^*, U_i, I_i)) + b_i \cdot (z_{i,i} \cdot U_i + I_i) \tag{49}$$

obtained by substituting (48) into (46), is locally solvable for x_i^* which corresponds to an isolated equilibrium point of the cell. This observation is true because i) for linear feedbacks $f_i(\xi_i) = K \cdot \xi_i$ with $K \in [\,k_1, k_2\,]$, (49) becomes

$$0 = \hat{A}_i \cdot x_i^* + \hat{U}_i \tag{50}$$

$$= [\,A_i + b_i \cdot w_{i,i} \cdot \frac{K}{1 - K \cdot w_{i,i} \cdot h_i} \cdot c_i^T\,] \cdot x_i^* + b_i \cdot (\,1 + w_{i,i} \cdot \frac{K}{1 - K \cdot w_{i,i} \cdot h_i} \cdot h_i\,) \cdot (z_{i,i} \cdot U_i + I_i)$$

ii). the nonsingularity of $\hat{A}_i$ is a necessary condition for the stability of the linear closed-loop system defined by

$$\dot{x}_i = \hat{A}_i \cdot x_i + \hat{U}_i \tag{51}$$

and iii) Since $\hat{A}_i$ is nonsingular for all $K \in [\,k_1, k_2\,]$, it follows from (40) and the local differentiability of the nonlinearity that (49) is locally uniquely solvable for x_i^*.

In conclusion, if the nonlinearity is differentiable in a neighborhood of an equilibrium point of a cell, then this equilibrium point should be isolated. In fact, the uniqueness of the equilibrium point is a necessary condition for global asymptotic stability. Therefore, the conditions (stated in Theorem 3) for the global asymptotic stability of a cell imply also the uniqueness of the solution of (46)-(47).

The conditions of Theorem 3 ensure global asymptotic stability not only for a particular cell, but also for any cell having a nonlinearity satisfying (38) and for any constant input. Hence, they will be

referred to as the absolute global asymptotic stability conditions.

Theorem 3 :

Consider an isolated cell described by (15)-(18). Suppose that the nonlinearity $f_i(\bullet)$ satisfies the incremental sector condition in (38) with finite constants k_1 , k_2 . The dynamical subcircuit is given by the transfer function

$$\hat{G}_i(s) = c_i^T \cdot [\,s\,I - A_i\,]^{-1} \cdot b_i + h_i$$

where, all eigenvalues of A_i have negative real parts and the pair (A_i, c_i) is observable, i.e.,

$$rank\ [\ c_i\ \ A_i^T \cdot c_i\ \ \cdots\ \ (A_i^T)^{n-1} \cdot c_i\ ] = t_i\ .$$

Under these conditions; for each constant input, the cell has a globally asymptotically stable equilibrium point $((x_i^*)^T, \xi_i^*)^T$ which is the unique solution of (46)-(47), if the following conditions are satisfied :

i) For inhibitory feedbacks $w_{i,i} < 0$;

$\hat{G}_i(s) \cdot e^{-s \cdot \tau_{ii}}$ satisfies one of the sets of conditions i)-iv) given in Lemma 1, but with $\alpha = -w_{i,i} \cdot k_1$, $\beta = -w_{i,i} \cdot k_2$ and $\hat{G}_i(s) \cdot e^{-s \cdot \tau_{ii}}$ instead of $\hat{G}_i(s)$.

ii) For excitatory feedbacks $w_{i,i} > 0$;

replace β by α and α by β ; and apply i) .

Proof :

Given a cell with constant input, let us derive first another cell with zero input such that an equilibrium point x_i^* of the given cell is globally asymptotically stable if and only if the equilibrium point 0 of the new cell is globally asymptotically stable. Let $((x_i^*)^T, \xi_i^*)^T$ be a solution to (46)-(47). By a change of variables, the system of equations in (15)-(18) can be transformed into the following system:

$$\dot{\bar{x}}_i(t) = A_i \cdot \bar{x}_i(t) + b_i \cdot \bar{e}_i(t) \tag{52}$$

$$\bar{\xi}_i(t) = c_i^T \cdot \bar{x}_i(t) + h_i \cdot \bar{e}_i(t) \tag{53}$$

$$\bar{y}_i(t) = F_i(\bar{\xi}_i(t)) = f_i(\bar{\xi}_i(t)+\xi_i^*) - f_i(\xi_i^*) \tag{54}$$

$$\bar{e}_i(t) = w_{i,j} \cdot \bar{y}_i(t - \tau_{i,j}) \tag{55}$$

where $\bar{x}_i(t) = x_i(t) - x_i^*$, $\bar{e}_i(t) = e_i(t) - e_i^*$, $\bar{y}_i(t) = y_i(t) - y_i^*$, $\bar{\xi}_i(t) = \xi_i(t) - \xi_i^*$,

$y_i^* = f_i(\xi_i^*)$ and $e_i^* = w_{i,j} \cdot y_i^* + z_{i,j} \cdot U_i + I_i$.

Observe that the transformed cell nonlinearity $F_i(\bullet)$ belongs to the sector $[k_1, k_2]$ since

$F_i(0) = f_i(\xi_i^*) - f_i(\xi_i^*) = 0$ and (38), with $\xi_i' = \bar{\xi}_i + \xi_i^*$, $\xi_i'' = \xi_i^*$, gives

$$k_1 \cdot \bar{\xi}_i^2 \le \bar{\xi}_i^2 \cdot F_i(\bar{\xi}_i) \le k_2 \cdot \bar{\xi}_i^2 . \tag{56}$$

In the sequel, we shall show that the equlibrium point 0 of the system in (52)-(55) is globally asymptotically stable. The proof parallels that of Theorem 6.4(1) in [9].

Equation (52) can be recast into the following form:

$$\bar{x}_i(t) = e^{A_i \cdot t} \cdot \bar{x}_i(0) + \int_0^t e^{A_i \cdot (t - \lambda)} \cdot b_i \cdot \bar{e}_i(\lambda) \cdot d\lambda . \tag{57}$$

Substituting (57) into (53), we obtain :

$$\bar{\xi}_i(t) = c_i^T \cdot e^{A_i \cdot t} \cdot \bar{x}_i(0) + \int_0^t c_i^T \cdot e^{A_i \cdot (t - \lambda)} \cdot b_i \cdot \bar{e}_i(\lambda) \cdot d\lambda + h_i \cdot \bar{e}_i(t) . \tag{58}$$

Observe that the system of equations in (58) and (54)-(55) defines a feedback system in the form of Figure 9 with the following inputs and outputs:

$$U_1(t) \equiv 0 \tag{59}$$

$$U_2(t) = c_i^T \cdot e^{A_i \cdot t} \cdot \bar{x}_i(0) \tag{60}$$

$$Y_1(t) = \bar{\xi}_i(t) - U_2(t) = \int_0^t c_i^T \cdot e^{A_i \cdot (t - \lambda)} \cdot b_i \cdot \bar{e}_i(\lambda) \cdot d\lambda + h_i \cdot \bar{e}_i(t) \tag{61}$$

$$Y_2(t) = w_{i,j} \cdot \bar{y}_i(t) . \tag{62}$$

Here, the subsystem G_1 is defined by the transfer function $\hat{G}_i(s) \cdot e^{-s \cdot \tau_{i,j}}$, and G_2 is defined by a memoryless nonlinearity $w_{i,j} \cdot F_i(\bullet)$.

The input $U_2(\bullet)$ belongs to L_2 because all eigenvalues of A_i have negative real parts. Since $U_1(\bullet)$ and $U_2(\bullet) \in L_2$ it follows from Lemma 1 that $Y_1(\bullet)$, $Y_2(\bullet)$ belongs to L_2 . Moreover,

$\bar{e}_i(t) = Y_2(t - \tau_{i,i})$ and the initial function $\theta_i(\bullet) \in L_2$ imply that $\bar{e}_i(\bullet) \in L_2$. It follows from $\bar{e}_i(\bullet) \in L_2$ and $\mathbf{c}_i^T \cdot e^{\mathbf{A}_i \cdot (\bullet)} \cdot \mathbf{b}_i \in L_2$ that

$$\int_0^t \mathbf{c}_i^T \cdot e^{\mathbf{A}_i \cdot (t - \lambda)} \cdot \mathbf{b}_i \cdot \bar{e}_i(\lambda) \cdot d\lambda \;\to\; 0 \qquad as \quad t \to \infty \tag{63}$$

For the proof of (63), see Theorem 6.4(1) in [9].

By (63), we have $Y_1(t) - h_i \cdot \bar{e}_i(t) \to 0$ as $t \to \infty$, and hence

$$\bar{\xi}_i(t) - U_2(t) - h_i \cdot w_{i,i} \cdot F_i(\bar{\xi}_i(t - \tau_{i,i})) \;\to\; 0 \qquad as \quad t \to \infty \tag{64}$$

It follows from (64) and $U_2(t) \to 0$ as $t \to \infty$ that, when t tends to infinity $\bar{\xi}_i(t)$ and $\bar{\xi}_i(t - \tau_{i,i})$ both tend to zero, and hence $Y_1(t)$ tends to zero. By the observability of the linear dynamical forward path, we conclude that $\bar{x}_i(t)$ tends to zero as $t \to \infty$. $\square$

Let us apply Theorem 3 to a 2 nd order cell.

Example 4 :

Consider a second order cell defined by

$$\dot{x}_i(t) = \begin{bmatrix} -2 & -1 \\ -1 & -1 \end{bmatrix} \cdot x_i(t) + \begin{bmatrix} 1 \\ 1 \end{bmatrix} \cdot e_i(t) \tag{65}$$

$$\xi_i(t) = \begin{bmatrix} 1 & 0 \end{bmatrix} \cdot x_i + 0 \cdot e_i(t) \tag{66}$$

$$y_i(t) = f_i(\xi_i(t)) = \frac{2}{\pi} \cdot V \cdot arctan(\frac{\pi}{2} \cdot \frac{K}{V} \cdot \xi_i(t)) \tag{67}$$

$$e_i(t) = 1 \cdot y_i(t) + 1 \cdot U_i + 0 \cdot I_i \tag{68}$$

Such a cell can be realized by the circuit shown in Figure 11a, where $x_i(t) = [\, v_{C1}(t) \,, v_{C2}(t) \,]^T$, $y_i(t) = v_0(t)$, and $C_1 = C_2$. One simple op amp implementation of this circuit is given in Figure 11b. The operational amplifier A1 is in the linear region [18]. The operational amplifier A2 is modeled by a nonlinear voltage-controlled voltage source such that its transfer characteristic is defined by (67) and

shown in Figure 11c. The circuit of Figure 11a is reduced into the well-known Wien bridge oscillator circuit when the input U_1 is zero.

Figure 11

It can be verified that $\hat{G}_1(s) = \dfrac{s}{s^2 + 3 \cdot s + 1}$ and that $f_1(\bullet)$ satisfies the incremental sector condition (38) with $k_1 = 0$, $k_2 = K$. By Theorem 3, we obtain the following inequality which gives a sufficient condition for the absolute global asymptotic stability of the equilibrium point 0 of the cell:

$$(1 - w^2)^2 + 3 \cdot w^2 \cdot (3 - K) > 0 \qquad \text{for } all \quad w \in \mathbf{R} \ . \tag{69}$$

We conclude that the cell is globally asymptotically stable, for each constant input U_1 , if $K < 3$. Note that, for this specific example, the conditions of Theorem 3 are weaker than the ones given in [21]. There, it is proved that the Wien bridge circuit is globally asymptotically stable if $K < 2$. By using the frequency domain Hopf bifurcation theorem given in [19], it was shown that the Wien bridge circuit is a locally stable nearly-sinusoidal oscillator when $K = 3 + \varepsilon$, where ε is a sufficiently small number. Cosequently, $K < 3$ is also a necessary condition for the absolute global asymptotic stability of the cell under consideration. □

Example 4 demonstrates that the conditions given by Theorem 3 are not conservative for the Wien bridge oscillator. Nevertheles, Theorem 3 gives only sufficient conditions. The following example will show that absolute global asymptotic stability holds for some generalized CNN even when the conditions of Theorem 3 are not satisfied.

Example 5 :

Consider an isolated cell of a CNN with constant input. Since the nonlinearity $f_1(\bullet)$ satisfies the incremental sector condition with $k_1 = 0$, $k_2 = 1$, it follows from Theorem 3, and the results in Example 4, that the region of absolute global asymptotic stability is the same that given for L_2-stability, as shown in Figure 10.

The conditions imposed on the feedback weights $w_{i,i}$ are also necessary for absolute stability when the feedback is excitatory. Indeed, by using the dynamic route approach [18], we can show that when $w_{i,i} > A$, an input with $|z_{i,i} \cdot U_i + I_i| < w_{i,i} - A$ can be found such that the cell has two stable equilibrium points and one unstable equilibrium point [1], [13]. For inhibitory feedbacks, when $-A < w_{i,i} < 0$, any cell with an arbitrary constant input is also globally asymptotically stable. This result follows from the dynamic route depicted in Figure 12, where $w_{i,i} < 0$. Observe that, for each input, the unique equilibrium point is globally asymptotically stable when $-A < w_{i,i} < 0$, even though this is not implied by Theorem 3. □

Figure 12

IV. STABILITY OF GENERALIZED CELLULAR NEURAL NETWORKS

In this section, we present several sets of results on the existence and uniqueness of the solutions, the boundedness of the trajectories, the input-output stability, and the global asymptotic stability, for the generalized CNN described by equations (1)-(4). In the stability analysis treated below, we shall present two different types of results. In the first type, the results are applied to the whole generalized CNN. In the second type, a generalized CNN is considered as an interconnection of individual cells, and the results are obtained in terms of the stability of the isolated cells and the connection characteristics, i.e., the connection topology and connection weights. This approach reduces the design of a class of generalized CNN with appropriate connection characteristics into the design of single cells. Moreover, it also provides a systematic and easy way to analyze a large scale generalized CNN in terms of its building blocks (individual cells) and the connection characteristics.

In the sequel, a generalized CNN described by the equations in (1)-(4), will be considered as a feedback system, as shown in Figure 13.

Figure 13

The forward path in Figure 13 consists of uncoupled, single-input, multiple-output, linear, time-invariant, distributed, dynamical systems. The feedback consists of a memoryless nonlinear system. The symbol t denotes the number of cells and the subscript $i \in \{1,2,....,t\}$ indices the cells. Note that the index i used here is different from the index $\mathbf{i} = (i_1, i_2, \ldots, i_n, k)$ which is used before. However, we can define a one-to-one map for transforming one set of index into another.

Existence and Uniqueness of Solutions :

It is a standard result in the theory of ordinary differential equations that there is a unique solution to (41) if $F(\bullet)$ is a Lipschitz continuous function. Unfortunately, this result can not be applied directly to generalized CNN since the set of equations (1)-(4) consists of a set of algebraic and differential-difference equations. Observe that this generalized CNN can be considered as a feedback system as shown in Figure 13. A rather general result for the existence and uniqueness of the solution of a feedback system is given in [8]. The following fact, which is stated for generalized CNN, is a special case of Theorem III.5.2 in [8].

Fact 1 :

Consider a generalized CNN described by (1)-(4). If each nonlinearity $f_i(\bullet)$ satisfies a global Lipschitz condition, i.e. , there exists a finite constant L_i such that

$$| f_i(\xi_i') - f_i(\xi_i'') | \leq L_i \cdot | \xi_i' - \xi_i'' | \quad \text{for } all \quad \xi_i', \xi_i'' \in \mathbf{R} \tag{70}$$

then, given the inputs $u_i(\bullet) \in L_{pe}$, there exists a unique set of $x_i(\bullet) \in L_{pe}^{t_i}$, $e_i(\bullet) \in L_{pe}$, $\xi_i(\bullet) \in L_{pe}$, and $y_i(\bullet) \in L_{pe}$ which satisfy (1)-(4). $\square$

It should be observed that the conditions of Fact 1 hold for CNN, HN, and any generalized CNN having differentiable nonlinearities, and any generalized CNN having continuous piecewise-linear non-linearities.

A Boundedness Result :

In the design of a physical circuit, it is naturally required that the circuit has bounded trajectories for any bounded input. Our next theorem gives a boundedness result, which is useful for the design of a generalized CNN.

Theorem 4 :

Consider a generalized CNN described by the equations in (1)-(4). Assume that all eigenvalues of each A_i have negative real parts, and each nonlinearity $f_i(\bullet)$ is bounded, i.e. ,

$$\| f_i(\bullet) \|_s = \sup_{\xi_i \in R} |f_i(\xi_i)| < \infty \tag{71}$$

where $\| \bullet \|_s$ is usually called the supremum norm. Under these conditions, if the inputs are bounded in the sense that

$$\| u_i(\bullet) \|_s = \sup_{t \in [0,\infty)} |u_i(t)| < \infty \tag{72}$$

then, every trajectory $[x_i^T(t), \xi_i(t)]^T$ of each cell is bounded in the sense that

$$\| x_i(\bullet) \|_s = \sup_{t \in [0,\infty)} \|x_i(t)\| < \infty$$

$$\| \xi_i(\bullet) \|_s = \sup_{t \in [0,\infty)} |\xi_i(t)| < \infty \tag{73}$$

where $\| \bullet \|$ denotes any vector norm.

Proof :

Applying the triangle inequality and (4), we obtain

$$|e_i(t)| \leq \sum_{i \in Y} |w_{i,i}| \cdot |y_i(t - \tau_{i,i})| + \sum_{i \in Y} |z_{i,i}| \cdot |u_i(t - \sigma_{i,i})| + |I_i| \tag{74}$$

It follows that

$$|e_i(t)| \leq \sum_{i \in Y} |w_{i,i}| \cdot \| f_i(\bullet) \|_s + \sum_{i \in Y} |z_{i,i}| \cdot \| u_i(\bullet) \|_s + |I_i| \tag{75}$$

The right hand side of (75) is independent of t. By this fact, together with (71)-(72), we obtain

$$\| e_i(\bullet) \|_s \leq \sum_{i \in Y} |w_{i,i}| \cdot \| f_i(\bullet) \|_s + \sum_{i \in Y} |z_{i,i}| \cdot \| u_i(\bullet) \|_s + |I_i| < \infty \quad . \tag{76}$$

The equation in (1) can be recast as follows:

$$x_i(t) = e^{A_i \cdot t} \cdot x_i(0) + \int_0^t e^{A_i \cdot (t - \lambda)} \cdot b_i \cdot e_i(\lambda) \cdot d\lambda \quad . \tag{77}$$

Applying the triangle inequality, we obtain

$$\| x_i(t) \| \leq \| e^{A_i \cdot t} \cdot x_i(0) \| + \int_0^t \| e^{A_i \cdot (t - \lambda)} \cdot b_i \| \cdot |e_i(\lambda)| \cdot d\lambda \quad . \tag{78}$$

Since all eigenvalues of A_i have negative real parts, there exist constants $c_1, c_2 > 0$, $a > 0$ such that

$$\| e^{A_i \cdot t} \cdot x_i(0) \| \leq c_1 \cdot e^{-a \cdot t} \qquad t \in [0, \infty)$$

$$\| e^{A_i \cdot t} \cdot b_i \| \leq c_2 \cdot e^{-a \cdot t} \qquad t \in [0, \infty) \ . \tag{79}$$

It follows from (78) and (79) that

$$\| x_i(t) \| \leq c_1 \cdot e^{-a \cdot t} + \frac{c_2}{a} \cdot (1 - e^{-a \cdot t}) \cdot \| e_i(\bullet) \|_\infty \tag{80}$$

and hence,

$$\| x_i(\bullet) \|_\infty \leq c_1 + \frac{c_2}{a} \cdot \| e_i(\bullet) \|_\infty \tag{81}$$

It follows from (81) and (76) that $x_i(\bullet)$ is bounded. The boundedness of $\xi_i(\bullet)$ follows by (2), (76) and (80). $\square$

It should be noted that the result given in (80) can be used also for computing an upper bound on $x_i(\bullet)$.

When the trajectories are bounded, every forward trajectory $[\, x^T(t), \xi(t) \,]^T$ approaches its positive limit set which is nonempty, closed, bounded and invariant [9]. Here, $[\, x^T(t), \xi(t) \,]^T$ denotes the vector of state variables $[\, (\, \cdots, x_i^T(t), \cdots \,), (\, \cdots, \xi_i(t), \cdots \,) \,]^T$. The positive limit set of a trajectory is the limit set of points p which are the limits of sequences $[\, x^T(t_k), \xi(t_k) \,]^T$ where $t_k \rightarrow +\infty$. If a generalized CNN is globally asymptotically stable, then the limit set of every trajectory consists of a single element which is necessarily the unique equilibrium point. For a bounded generalized CNN, the positive limit set of a trajectory may contain cycles or more complicated orbits.

The conditions of Theorem 4 are not only sufficient for boundedness of generalized CNN, but also sufficient for eventually uniform boundedness, which is stronger than mere boundedness [17]. By the eventually uniform boundedness of a generalized CNN, we mean that, given any bounded input, there exists a closed and bounded set such that any trajectory enters and remains inside it for all time $t \geq T$, where $T < \infty$ may depend on the initial conditions. The fact that a generalized CNN which satisfies the conditions of Theorem 4 is eventually uniformly bounded, can be shown as follows. The only term in (80) which depends on the initial conditions is $c_1 \cdot e^{-a \cdot t}$. This term can be made sufficiently small by choosing a large t since $a > 0$. Therefore, we can find a time $T < \infty$ and a set to prove the eventually uniform boundedness of the generalized CNN.

L$_2$- stability :

In the sequel, we shall present two types of L_2-stability results for generalized CNN. The first type of results, stated by Theorem 5, gives conditions which are applied to the whole generalized CNN. This result is more general than the second result, but it does not exploit the L_2-stability of the individual cells. The second type of results, which will be derived from Theorem 5, is in terms of the L_2-stability of the isolated cells and the connection characteristics.

Theorem 5 is based on Lemma 3, a special case of Theorem V.2.4 in [8], which provides a sufficient condition for the L_2-stability of the general multivariable feedback system shown in Figure 9.

Lemma 3 [8] :

Consider the feedback system shown in Figure 9, where $U_1(t)$, $U_2(t)$, $E_1(t)$, $E_2(t)$, $Y_1(t)$ and $Y_2(t) \in \mathbf{R}^l$. The subsytem G_1 consists of a set of uncoupled, linear, time-invariant, possibly distributed, scalar input, scalar output, dynamical systems. It is described by a diagonal transfer matrix $\hat{G}_1(s)$ with the diagonal elements $\hat{g}_i(s) = \dfrac{\hat{n}_i(s)}{\hat{d}_i(s)} \cdot e^{-s\tau_i}$, where $\hat{n}_i(s)$ and $\hat{d}_i(s)$ are polynomials with no common zeros and the inverse Laplace transform of $\hat{g}_i(s)$ belongs to L_{pe} . The subsytem G_2 is memoryless and represented by

$$Y_2(t) = \Psi[E_2(t)] \tag{82}$$

where $\Psi(\bullet) : \mathbf{R}^l \to \mathbf{R}^l$ satisfies (83) with a constant matrix $K \in \mathbf{R}^{l \times l}$ and a real constant γ .

$$\| \Psi(\xi) - K \cdot \xi \| \leq \gamma \cdot \| \xi \| \quad \text{for } all \quad \xi \in \mathbf{R}^l \quad . \tag{83}$$

Under these conditions, if

i) $\quad \inf\limits_{Re\, s \geq 0} | \det [I + K \cdot \hat{G}_1(s)] | > 0 \quad , \tag{84}$

ii) $\quad \det [\, diag(\hat{d}_1(s), \ldots, \hat{d}_l(s)) + K \cdot diag(\hat{n}_1(s) \cdot e^{-s\tau_1}, \ldots, \hat{n}_l(s) \cdot e^{-s\tau_l}) \,] \neq 0$

$\quad whenever \quad Re\, s \geq 0 \quad \text{and} \quad \prod\limits_{i=1}^{l} \hat{d}_i(s) = 0 \quad , \tag{85}$

iii) $\quad \gamma \cdot \{ \sup\limits_{w \in \mathbf{R}} \max\limits_{i} \lambda_i [\, \hat{H}_K^*(jw) \cdot \hat{H}_K(jw) \,] \}^{\frac{1}{2}} < 1 \tag{86}$

where M^* denotes the conjugate transpose of the matrix M , $\lambda_i (M)$ denotes the i th eigenvalue of the matrix M , and

$$\hat{H}_K(s) = \hat{G}_1(s) \cdot [\ \mathbf{I} + \mathbf{K} \cdot \hat{G}_1(s)\ ]^{-1}\ , \tag{87}$$

then, the system is L_2-stable. $\square$

The inequality in (84) can be checked by a Nyquist graphical test as done in Lemma 1. The graphical test is based on Fact 2.

Fact 2 [8] :

The inequality in (84) holds if and only if

i) $\det[\ \mathbf{I} + \mathbf{K} \cdot \hat{G}_1(jw)\ ] = 1 + \hat{g}(jw) \neq 0$ for *all* $w \in \mathbf{R}$, $\tag{88}$

ii) $\Delta\,\theta = \lim\limits_{\Omega \to \infty} [\ \theta(j\Omega) - \theta(-j\Omega)\ ] = \sum\limits_{k} \mu_k = n_k$ $\tag{89}$

where $\theta(jw)$ is the phase of $1 + \hat{g}(jw)$, i.e., $\theta(jw) = arg\ [\ 1 + \hat{g}(jw)\ ]$; n_p denotes the number of poles in the open right half-plane; and μ_k is the multiplicity of the k'th pole. $\square$

Condition (88) means that $\hat{g}(jw)$ is bounded away from $-1 + j \cdot 0$. Condition (89) can be interpreted as follows: The Nyquist diagram of $\hat{g}(s)$ [i.e., the graph of the map $w \to \hat{g}(jw)$] encircles the point, $-1 + j \cdot 0$, n_p times in the counterclockwise direction.

Now, we shall apply Lemma 3 to generalized CNN.

Theorem 5 :

Consider the generalized CNN shown in Figure 13. Assume that all nonlinearities $f_i(\bullet)$ belong to a closed sector $[\ k_1, k_2\ ]$ with finite constants k_1, k_2 . Assume the output $y_i(t)$ of any cell $C_{i'}$ is received, by all neighbor cells, with the same delay, i.e., for each $C_{i'}$, there exists a $\tau_{i'}$ such that $\tau_{i\ ,i'} = \tau_{i'}$ for all i . Then, th generalized CNN is L_2-stable if the conditions in (83)-(86) are satisfied with

$$\hat{G}_1(s) = diag\ (\ \hat{G}_1(s) \cdot e^{-s\tau_1}\ ,\dots,\ \hat{G}_i(s) \cdot e^{-s\tau_i}\ )\ , \tag{90}$$

$$\mathbf{K} = (\frac{-k_2 - k_1}{2}) \cdot \mathbf{W}\ , \tag{91}$$

$$\gamma = |\ \frac{k_2 - k_1}{2}\ | \cdot \|\ \mathbf{W}\ \| \tag{92}$$

where, $\hat{G}_i(s) = \mathbf{c}_i^T \cdot [\ s\ \mathbf{I} - \mathbf{A}_i\ ]^{-1} \cdot \mathbf{b}_i + h_i$, $\mathbf{W}$ is the matrix whose elements are the connection weights $\mathbf{W}_{i,i'}$, and $\|\ \mathbf{W}\ \|$ denotes any induced norm of the matrix $\mathbf{W}$.

Proof:

By our assumption on the delay times, the generalized CNN shown in Figure 13 can be reduced into the feedback system of Figure 9. Then the proof follows from Lemma 3 and the fact that (29) together with (91)-(92) implies (83). □

Theorem 5 can also be applied to a generalized CNN having nonlinearities belonging to different sectors. To do this, we can simply define a sector covering all sectors to which the nonlinearities belong.

Let us now apply Theorem 5 to a CNN.

Example 6 :

By the definition of CNN, we obtain $\hat{G}_1(s) = \frac{1}{s+A} \cdot I$, $K = -\frac{1}{2} \cdot W$, and $\gamma = \frac{1}{2} \cdot \| W \|$. We can rewrite conditions (84) as

$$\inf_{\text{Re} s \geq 0} |\det [I - \frac{1}{2} \cdot \frac{1}{s+A} \cdot W]| = \inf_{\text{Re} s \geq 0} \frac{1}{|s+A|} \cdot \prod_{i=1}^{t} | s + A - \frac{1}{2} \cdot \lambda_i(W) | > 0 \quad (93)$$

where $\lambda_i(W)$ denotes the i th eigenvalue of the connection matrix W. Observe that (93) holds if and only if

$$\text{Re} \{ \lambda_i(W) \} < 2 \cdot A \qquad \text{for } all \ i \ . \quad (94)$$

For a CNN, (85) becomes

$$\det [(s+A) \cdot I - \frac{1}{2} \cdot W] \neq 0 \quad whenever \ \text{Re} s \geq 0 \text{ and } (s+A) = 0 \quad (95)$$

which is equivalent to the nonsingularity of the connection matrix W, i.e.,

$$\det W \neq 0 \quad (96)$$

The inequality in (86) can be recast as

$$\sup_{w \in R} \max_{i} \{ \frac{1}{\lambda_i(M_K)} \} < \frac{4}{\| W \|^2} \quad (97)$$

where

$$M_K = [(A^2 + w^2) \cdot I - \frac{A - jw}{2} \cdot W - \frac{A + jw}{2} \cdot W^T + \frac{1}{4} \cdot W \cdot W^T] \quad (98)$$

and $\lambda_i(M_K)$ is the i th eigenvalue of M_K. The equivalence of (86) and (97) follows from the facts that $\hat{H}_K^*(jw) \cdot \hat{H}_K(jw)$ has positive real eigenvalues only and its eigenvalues can be given as

$$\frac{1}{\lambda_i \, (\mathbf{M}_K)} \; .$$

We conclude that if the connection matrix $\mathbf{W}$ satisfies the conditions in (94), (96) and (97), then the associated CNN is L_2-stable. $\square$

Note 1 :

Theorem 1, which gives the conditions for the L_2-stability of an isolated cell, is indeed a special case of Theorem 5. For an isolated cell C_i, the condition in (84), (85) and (86) takes the form in (99), (100) and (101), respectively.

$$\operatorname*{Inf}_{\substack{\mathrm{Re}\, s \,\geq\, 0}} \; | \, 1 - (\frac{k_1 + k_2}{2}) \cdot \mathbf{W}_{i,i} \cdot \hat{g}_i(s) \, | \; > \; 0 \quad . \tag{99}$$

$$(\frac{k_1 + k_2}{2}) \cdot \mathbf{W}_{i,i} \cdot \hat{n}_i(s) \cdot e^{-s \, \cdot \, \tau_i} \; \neq \; 0 \quad \textit{whenever} \quad \mathrm{Re}\, s \geq 0 \quad . \tag{100}$$

$$\operatorname*{sup}_{w \,\in\, \mathbf{R}} \; \frac{| \, \hat{g}_i(jw) \, |}{| \, 1 - (\frac{k_1 + k_2}{2}) \cdot \mathbf{W}_{i,i} \cdot \hat{g}_i(jw) \, |} \; < \; \frac{2}{\lceil k_2 - k_1 \rceil \cdot | \mathbf{W}_{i,i} |} \quad . \tag{101}$$

It is shown in [8], by using Fact 1, that the conditions in (99)-(101) can be checked by the Nyquist graphical test stated in Lemma 1. $\square$

Our next result gives a connection topology underwhich L_2-stable subnetworks yield an L_2-stable network.

Fact 3 :

Consider a generalized CNN Φ_m^n consisting of a cascade of the layers Π_l^k . Let us isolate each layer from the other layers by setting all extra-level connection weights to zero. If each isolated layer is L_p-stable, then so is the whole generalized CNN Φ_m^n .

Proof :

The proof follows directly from the definition of a cascade generalized CNN. $\square$

Our next theorem describes that, for some suitable values of the connection weights, the interconnection of a class of L_2-stable individual cells is also L_2-stable.

Note 2 :

It will be assumed in Theorem 6 that each individual cell satisfies the conditions of Theorem 5 (and equivalently of Theorem 1) but with the condition (101) replaced by the following stronger condition :

$$\sup_{w \in R} \frac{|\hat{g}_i(jw)|}{|1 - (\frac{k_1 + k_2}{2}) \cdot W_{i,i} \cdot \hat{g}_i(jw)|} < \frac{2}{|k_2 - k_1| \cdot |W_{i,i}| \cdot \rho} \tag{102}$$

where $\rho = \frac{\|W\|}{\min_i |\lambda_i(W)|}$. It is known [8] that $\rho \geq 1$ for any induced matrix norm $\|W\|$. This

implies that if (102) holds, then (101) holds. Condition (102) can be checked graphically in a way similar to the graphical test in Lemma 1. To do this, observe the following facts:

For the complex number $z = \hat{g}_i(jw)$,

i) If $|k_2 + k_1| > \rho \cdot |k_2 - k_1|$, then (102) is equivalent to the condition that z is bounded away from the disk $\hat{D}$ (which is a circle in the complex plane centered on the real axis and passing through the points $\frac{2}{[k_2 + k_1 + \rho \cdot (k_2 - k_1)] \cdot W_{i,i}} + j \cdot 0$ and

$\frac{2}{[k_2 + k_1 - \rho \cdot (k_2 - k_1)] \cdot W_{i,i}} + j \cdot 0$),

ii) If $|k_2 + k_1| < \rho \cdot |k_2 - k_1|$, then (102) is equivalent to the condition that z is in the interior of the disk $\hat{D}$ given in i),

and iii) If $|k_2 + k_1| = \rho \cdot |k_2 - k_1|$, then (102) is equivalent to the condition that $(k_2 + k_1) \cdot W_{i,i} \cdot \mathrm{Re}\, z < 1$. $\square$

Theorem 6 :

Consider the generalized CNN shown in Figure 13. Assume that i) There is a nonempty set $I \subseteq R$ such that for $W_{i,i} \in I$, each individual cell, isolated from the rest of the generalized CNN, satisfies the conditions of Theorem 5 but with the condition in (102) instead of (101), ii) the output of a cell C_i is transmitted to the neighbor cells with the same delay τ_i ; and iii) all cells are identical, i.e., they have the same nonlinearity and the same transfer function $\hat{g}(s)$ defined by

$$\hat{g}(s) = \frac{\hat{n}(s)}{\hat{d}(s)} \cdot e^{-s\tau} = [c^T \cdot [sI - A]^{-1} \cdot b + h] \cdot e^{-s\tau} \tag{103}$$

with $c = c_i$, $A = A_i$, $b = b_i$, $h = h_i$, $\tau = \tau_i$ for all $i \in \{1,2,...,t\}$; and $\hat{n}(s)$ does not have a zero in the closed right half-plane. Under these conditions, the generalized CNN is L_2-stable

if

i) The connection matrix W is nonsingular and symmetric,

and ii) Any eigenvalue $\lambda_i(W)$ lies in I .

Proof :

The assumption on the delay times allows us to use Theorem 5. We will now show the conditions in (84)-(86) are satisfied. For the generalized CNN considered, (84) becomes (104).

$$\inf_{\substack{Re\ s \geq 0}} \ |\det[\ I - (\frac{k_2 + k_1}{2}) \cdot W \cdot \hat{g}(s)\ ]|$$
$$= \inf_{\substack{Re\ s \geq 0}} \prod_{i=1}^{t} \ |\ 1 - (\frac{k_2 + k_1}{2}) \cdot \lambda_i(W) \cdot \hat{g}(s)\ | \ > \ 0 \quad . \quad (104)$$

Each term in the product of (104) corresponds to the condition for an isolated cell. The inequality in (104) holds since each isolated cell satisfies the condition in (99) and each $\lambda_i(W)$ lies in I .

For the generalized CNN under consideration, the condition (85) assumes the following form :

$$\det[\ \hat{d}(s) \cdot I - (\frac{k_2 + k_1}{2}) \cdot W \cdot \hat{n}(s)\ ] \ \neq \ 0 \quad whenever \ \ Re\ s \geq 0 \ \ and \ \ \hat{d}(s) = 0 . \quad (105)$$

Condition (105) holds because $\hat{d}(s)$ does not have zeros in the right half-plane and the connection matrix W is nonsingular.

Observe next that $\hat{H}_K(s)$ as defined in (87) can be recast as follows :

$$\hat{H}_K(s) = \hat{g}(s) \cdot [\ I - (\frac{k_2 + k_1}{2}) \cdot W \cdot \hat{g}(s)\ ]^{-1} \quad . \quad (106)$$

Our next relation follows by the symmetry of the connection matrix W .

$$\lambda_i \{\ \hat{H}_K(jw)^* \cdot \hat{H}_K(jw)\ \} = \frac{|\ \hat{g}(jw)\ |^2}{|\ 1 - (\frac{k_2 + k_1}{2}) \cdot \lambda_i(W) \cdot \hat{g}(jw)\ |^2} \quad . \quad (107)$$

Now, the inequality in (86) takes the form in (108).

$$\sup_{w \in R} \ \max_i \ \frac{|\ \hat{g}(jw)\ |}{|\ 1 - (\frac{k_2 + k_1}{2}) \cdot \lambda_i(W) \cdot \hat{g}(jw)\ |} \ < \ \frac{2}{|k_2 - k_1| \cdot \|\ W\ \|} \quad . \quad (108)$$

Condition (108) holds since each cell satisfies condition (102) and since each $\lambda_i(W)$ lies in I . $\square$

The following corollary is a direct consequence of Fact 2 and Theorem 6.

Corollary 1 :

Consider a generalized CNN Φ_m^n made up of a cascade of the layers Π_l^n . If each isolated layer Π_l^n satisfies the conditions of Theorem 6, then the whole generalized CNN Φ_m^n is L_2-stable.

Proof :

The L_2-stability of each isolated layer follows by Theorem 6. Then, Fact 2 completes the proof.

□

L_∞– stability :

We now present, by Theorems 7 and 8, sufficient conditions for the L_∞-stability of generalized CNN. Theorems 7 and 8 are based on Lemma 4 which is a generalization of Lemma 2 and a direct consequence of Theorem V.2.4 and Lemma V.3.21 in [8].

Lemma 4 :

Consider the feedback system shown in Figure 9, where $U_1(t)$, $U_2(t)$, $E_1(t)$, $E_2(t)$, $Y_1(t)$, $Y_2(t) \in R^l$ and $U_2(t) \equiv 0$. The subsystem G_1 consists of a set of uncoupled, linear, time-invariant, possibly distributed, scalar input, scalar output, dynamical systems. The subsystem G_1 is described by a diagonal transfer matrix $\hat{G}_1(s)$ with the diagonal elements $\hat{g}_i(s) = \dfrac{\hat{n}_i(s)}{\hat{d}_i(s)} \cdot e^{-s\tau_i}$,

where, $\hat{n}_i(s)$ and $\hat{d}_i(s)$ are polynomials with no common zeros and the inverse Laplace transform $g_i(t)$ of $\hat{g}_i(s)$ satisfies the exponential weighting condition:

$e^{at} \cdot g_i(t) \in L_1 \cap L_2$ for *some* $a > 0$.

The subsystem G_2 is memoryless and represented by $Y_2(t) = \Psi[E_2(t)]$, where, $\Psi(\bullet) : R^l \to R^l$ satisfies (83).

Under these conditions, if the a-shifted transfer function $\hat{G}_1(-a + s)$ satisfies the conditions in (84)-(86), then $U_1(\bullet) \in L_\infty^l$ implies that $E_1(\bullet)$, $Y_1(\bullet) \in L_\infty^l$. □

Let us apply next Lemma 4 to generalized CNN.

Theorem 7 :

Consider the generalized CNN shown in Figure 13. Assume that each $\hat{G}_1(s)$ is strictly proper

and that all of its poles p_j have negative real parts. If the conditions of Theorem 5 hold but with an a-shifted transfer function $\hat{G}_1(-a + s)$ (here, $a \geq -\operatorname{Re} p_j > 0$), then the generalized CNN is L_∞-stable.

Proof:

The proof is similar to that of Theorem 2, where Lemma 4 is used. □

The conditions of Theorem 7 can be verified by examining the transfer function of the whole generalized CNN. In contrast, the conditions of Theorem 8 can be checked by examining the connection characteristics alone, if the individual cells satisfies certain conditions.

Theorem 8:

Consider a generalized CNN Φ_m^n made up of a cascade of the layers Π_l^k. Assume that each isolated cell of a layer Π_l^k has the same transfer function $\hat{g}(s)$ defined in (103), where, $\dfrac{\hat{n}(s)}{\hat{d}(s)}$ is strictly proper and all of its poles p_j have negative real parts. Then the generalized CNN Φ_m^n is L_∞-stable, if each isolated layer Π_l^k satisfies the conditions of Theorem 6 but with an a-shifted transfer function $\hat{g}(-a + s)$ (here, $a \geq -\operatorname{Re} p_j > 0$).

Proof:

The proof follows from Fact 3 and Theorems 5-7. □

Global Asymptotic Stability:

Let us now generalize the results, obtained in section III, on the global asymptotic stability of the individual cells, into the whole generalized CNN. Theorem 9 shows that the conditions given by Theorem 5 for the L_2-stability of generalized CNN also ensure the global asymptotic stability of the generalized CNN, if the nonlinearities $f_i(\bullet)$ satisfies a condition stronger than the sector condition. Theorem 10 presents a set of conditions on the connection characteristics which guaranties that the interconnection of a class of globally asymptotically stable individual cells yields a globally asymptotically stable generalized CNN.

Throughout the global asymptotic stability, we assume that i) the external inputs $u_i(t)$ are con-

stants and denoted by U_i , ii) all nonlinearities $f_i(\bullet)$ satisfy the incremental sector condition in (38) with finite constants k_1, k_2 , iii) the set of differential-difference equations in (1)-(4) has a unique equilibrium point. As discussed in section III, the last assumption is not an extra condition for a globally asymptotically stable system. The second assumption, which is needed for the global asymptotic stability of a generalized CNN under an arbitrary constant input, ensures the existence and uniqueness of the solutions to the equations in (1)-(4). This follows from Fact 1 and the result in (39).

Theorem 9 :

Consider the generalized CNN shown in Figure 13. Suppose that all nonlinearities $f_i(\bullet)$ satisfy the incremental sector condition in (38) with the same finite constants k_1, k_2 , and assume the output $y_i(t)$ of any cell C_i is received by neighbor cells with the same delay $\tau_i = \tau_{i,i'}$. For the linear dynamical subcircuits in the forward path having the following transfer function

$$\hat{G}_i(s) = c_i^T \cdot [\, s\, I - A_i\,]^{-1} \cdot b_i + h_i$$

assume all eigenvalues of A_i have negative real parts and assume the pair (A_i , c_i) is observable. Under these conditions, if $\hat{G}_1(s)$ together with K and γ defined in (90)-(92) satisfy the conditions in (83)-(86), then, for each constant input, the generalized CNN has a unique equilibrium point which is globally asymptotically stable.

Proof :

The proof is parallel to that of Theorem 3 and follows by Theorem 5. □

In the sequel, we shall present a class of generalized CNN where the global asymptotic stability of individual cells implies the global asymptotic stability of the whole generalized CNN, under some suitable interconnection characteristics. This result needs Fact 4 which gives a connection topology ensuring that the interconnection of the globally asymptotically stable layers is also globally asymptotically stable. For a proof of Fact 4, see Theorem 5 in [2].

Fact 4 :

Consider a generalized CNN Φ_m^n made up of a cascade of the layers Π_l^k . If each isolated layer Π_l^k is globally asymptotically stable, then so is the whole generalized CNN Φ_m^n . □

Theorem 10 :

Consider a generalized CNN Φ_m^n made up of a cascade of the layers Π_i^g . Assume that i) for each layer Π_i^g , all nonlinearities $f_i(\bullet)$ satisfy the incremental sector condition in (38) with the same finite constants k_1, k_2 , ii) each layer Π_i^g , as a feedback system shown in Figure 13, satisfies the conditions of Theorem 13, where all eigenvalues of A have negative real parts, and the pair (A, c) is observable. Then, for each constant input, the generalized CNN Φ_m^n has a unique equilibrium point which is globally asymptotically stable.

Proof :

The proof follows from Fact 4, Theorem 9, and uses the same approach as that of Theorem 6. $\square$

V. CONCLUSION

A new neural network architecture, generalized CNN, has been developed. generalized CNN is a very general neural network model in regards to both connection topology and structure of building blocks. Hence, the potential applications of generalized CNN go well beyond the ones offered by the common neural networks consisting of simple cells. In particular, the results given for the global asymptotic stability, and the input-output stability of the generalized CNN, can be used for designing generalized CNNs as computing and/or cognitive machines.

VI. REFERENCES

[1]   L. O. Chua and L. Yang ," Cellular neural networks: theory and applications," IEEE Trans. Circuits Syst. Vol.35, pp.1257-1290, October 1988.

[2]   M. W. Hirch ," Convergent activation dynamics in continuous time networks," Neural Networks, Vol.2, pp.331-349, 1989.

[3]   M. Cohen and S. Grossberg ," Absolute stability of global pattern formation and parallel memory storage by competitive neural networks," IEEE Trans. Systems, Man and Cybernetics, SMC-13,

pp.815-826, 1983.

[4]   J. J. Hopfield ,"Neurons with graded response have collective computational properties like those of two-state neurons," Proceedings of the National Academy of Sciences, USA, Vol.81, pp.3088-3092, 1984.

[5]   M. Minsky and S. Papert, Perceptrons, The MIT press, Cambridge, MA, 1969.

[6]   Y. Yao and W. J. Freeman, "Model of biological pattern recognition with spatially chaotic dynamics," Neural Networks, Vol.3, pp.153-170, 1990.

[7]   K. S. Narendra and J. H. Taylor , Frequency Domain Criteria for Absolute Stability. New York , Academic, 1973.

[8]   C. A. Desoer and M. Vidyasagar, Feedback Systems : Input-Output Properties. New York. Academic. 1975.

[9]   M. Vidyasagar , Nonlinear Systems Analysis. Prentice-Hall. New Jersey. 1978.

[10]   D. G. Kelly , "Stability in contractive nonlinear neural networks," IEEE Trans. Biomedical Engineering, Vol.37, No.3, pp.231-242 March 1990.

[11]   I. W. Sandberg," Some theorems on the dynamic response of nonlinear transistor networks," Bell Syst. Tech. J. Vol.48, No.1, pp.35-54, January 1969.

[12]   L. O. Chua and T. Roska ," Stability of a class of nonreciprocal cellular neural networks," IEEE Trans. Circuits Syst. Vol.37 , No.11, November 1990.

[13]   L. O. Chua and B. E. Shi ," Exploiting cellular automata in the design of cellular neural networks for binary image processing," Memorandum, No. UCB/ERL M89/130, November 1989.

[14]   A. N. Michel, J. A. Farrel and W. Porod ,"Qualitative analysis of neural networks," IEEE Trans. Circuits Syst., Vol.36, No.2, pp.229-243, February 1989.

[15]   A. Dembo, O. Farotimi and T. Kailath, "High-order absolutely stable neural networks," IEEE Trans. Circuits Syst., Vol.38, No:1, pp.57-65, January 1991.

[16]   L. O. Chua, M. Komuro and T. Matsumoto ,"The double scroll family," IEEE Trans. Circuits Syst. , Vol. CAS-33, pp.1073-1118, November 1986.

[17] L. O. Chua ,"Dynamic nonlinear networks: state-of-the-art," IEEE Trans. Circuits Syst. Vol. CAS-27, No.11, pp.1059-1087, November 1980.

[18] L. O. Chua, C. A. Desoer and E. S. Kuh , Linear and Nonlinear Circuits, McGraw-Hill, NewYork, 1987.

[19] A. I. Mees and L. O. Chua ," The Hopf bifurcation theorem and its applications to nonlinear oscillations in circuits and systems," IEEE Trans. Circuits Syst. Vol. CAS-26, No.4, pp.235-254, April 1979.

[20] R. D. Driver , Ordinary and Delay Differential Equations, Applied Mathematical Sciences, V.20, Springer-Verlag, NewYork, 1977.

[21] L. O. Chua and D. N. Green ," A qualitative analysis of the behavior of dynamic nonlinear networks: stability of autonomous networks," IEEE Trans. Circuits Syst., Vol. CAS-23, No.6, pp.355-379, June 1976.

CAPTIONS FOR FIGURES

Figure 1. A 2-dimensional 3-layer GCNN, Ω_3^2 . Each layer has nearest neighbor intra-layer interconnection of size r=1, while every two successive layers are fully-interconnected, for instance, each cell of Π_2^2 is connected to every cell in layer Π_1^2 and Π_3^2 .

Figure 2. a) A feedforward GCNN Γ_3^1 , b) A cascade GCNN Φ_3^1 , and c) A recurrent GCNN.

Figure 3. The connectivity of a single cell within the same layer k for a) $r_{k,k} = 1$ and

$d_{k,k} (i_1, i_2, k; \hat{i}_1, \hat{i}_2, k) = |i_1 - \hat{i}_1| + |i_2 - \hat{i}_2|$,   b) $r_{k,k} = 1$ and

$d_{k,k} (i_1, i_2, k; \hat{i}_1, \hat{i}_2, k) = \max \{ |i_1 - \hat{i}_1| , |i_2 - \hat{i}_2| \}$ and   c) $r_{k,k} = 2$ and

$d_{k,k} (i_1, i_2, k; \hat{i}_1, \hat{i}_2, k) = |i_1 - \hat{i}_1| + |i_2 - \hat{i}_2|$.

Figure 4. The extra-level connectivity of a single cell of a 1-dimensional 2-layer GCNN with a)

$r_{k,k+1} = 1$ and $d_{k,k+1} (i, k ; \hat{i}, k+1) = |i_1 - \hat{i}_1| + 1$ and   b) $r_{k,k+1} = 1$ and

$d_{k,k+1} (i, k ; \hat{i}, k+1) = \max \{ |i_1 - \hat{i}_1|, 1 \}$, respectively.

Figure 5. Block diagram of a cell.

Figure 6. Feedback diagram of an isolated cell.

Figure 7. a) Chua's circuit consisting of a linear passive resistor, a linear inductor, two linear capacitors, and one nonlinear resistor. b) The v-i characteristic of the nonlinear resistor R_N .

Figure 8. The region where the function belonging to the sector $[k_1 , k_2]$ lies.

Figure 9. Block diagram of a general nonlinear feedback system.

Figure 10. The region of L_2-stability for an isolated cell of a CNN obtained by the circle criterion.

Figure 11. a) A circuit model of an oscillatory second order cell. b) The Wien bridge oscillator circuit.

c) The transfer function of the voltage-controlled source.

Figure 12. The dynamic route for an isolated cell of a CNN when $w_{1J} < 0$.

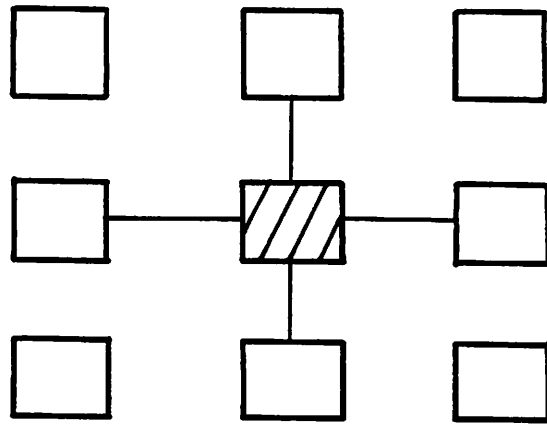**Figure 13.** A GCNN considered as a multivariable feedback system.
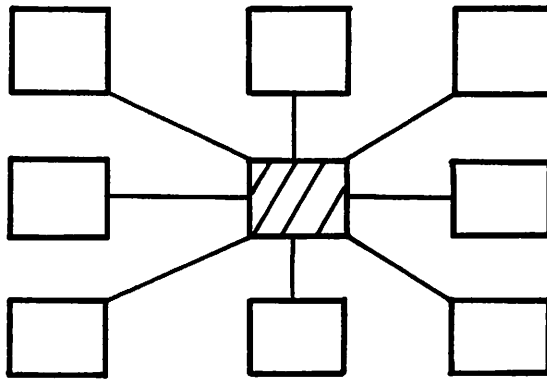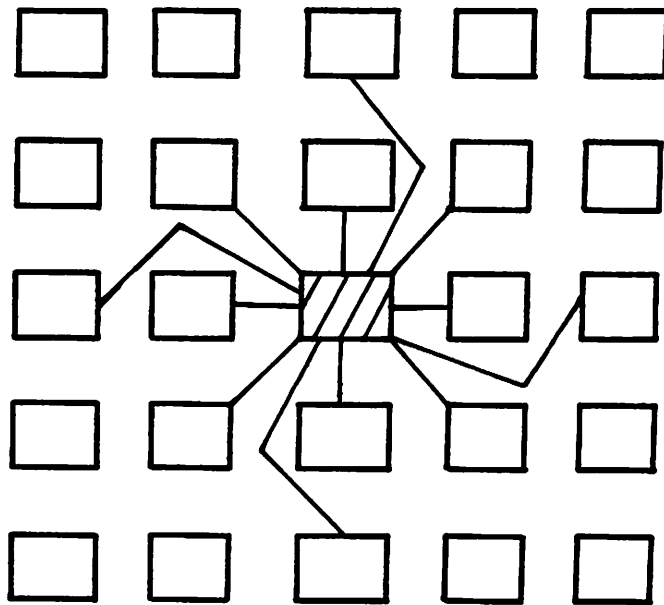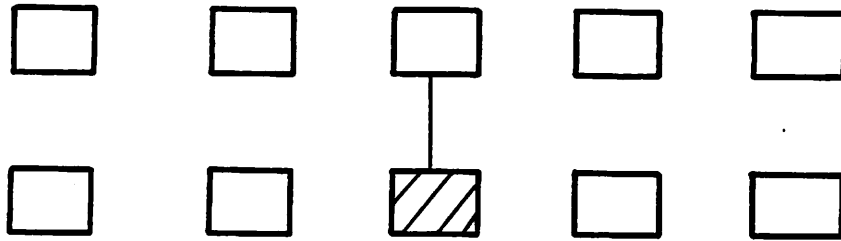
π_3^2

π_2^2
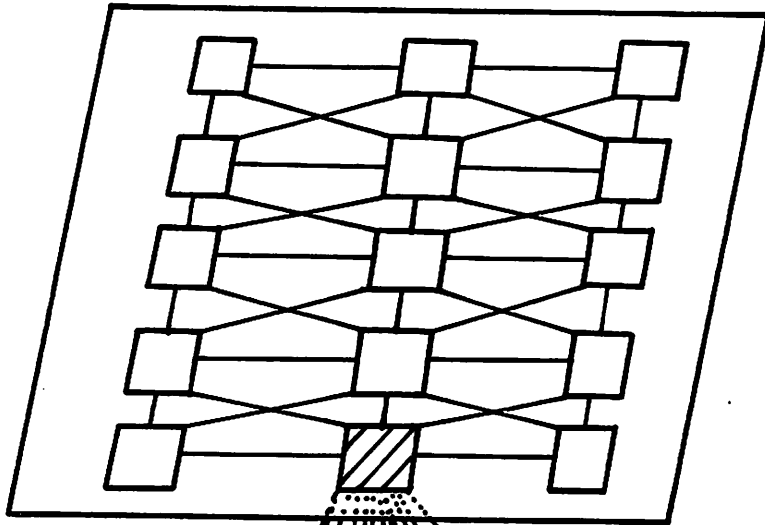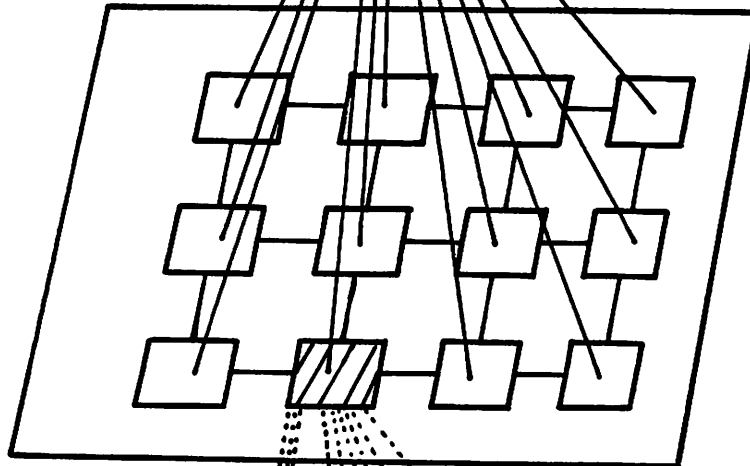
π_1^2
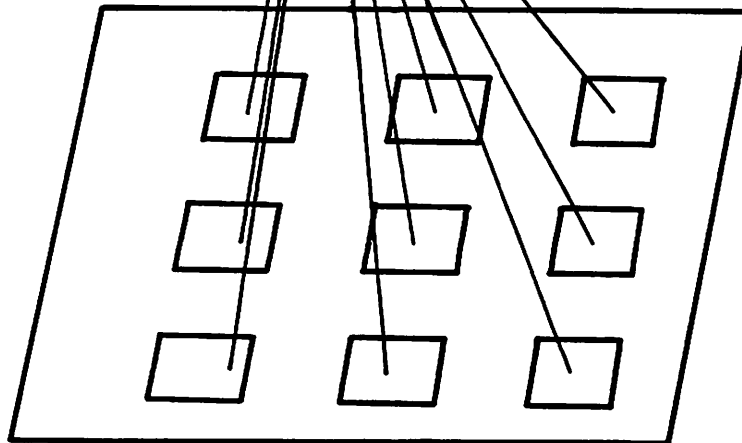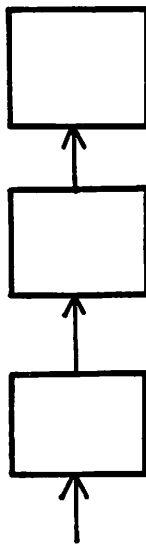
FIGURE 1

(a)
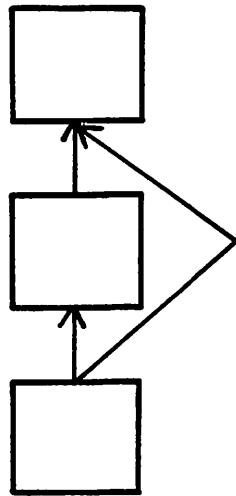
(b)
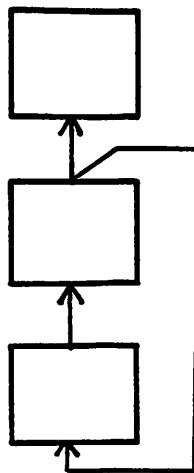
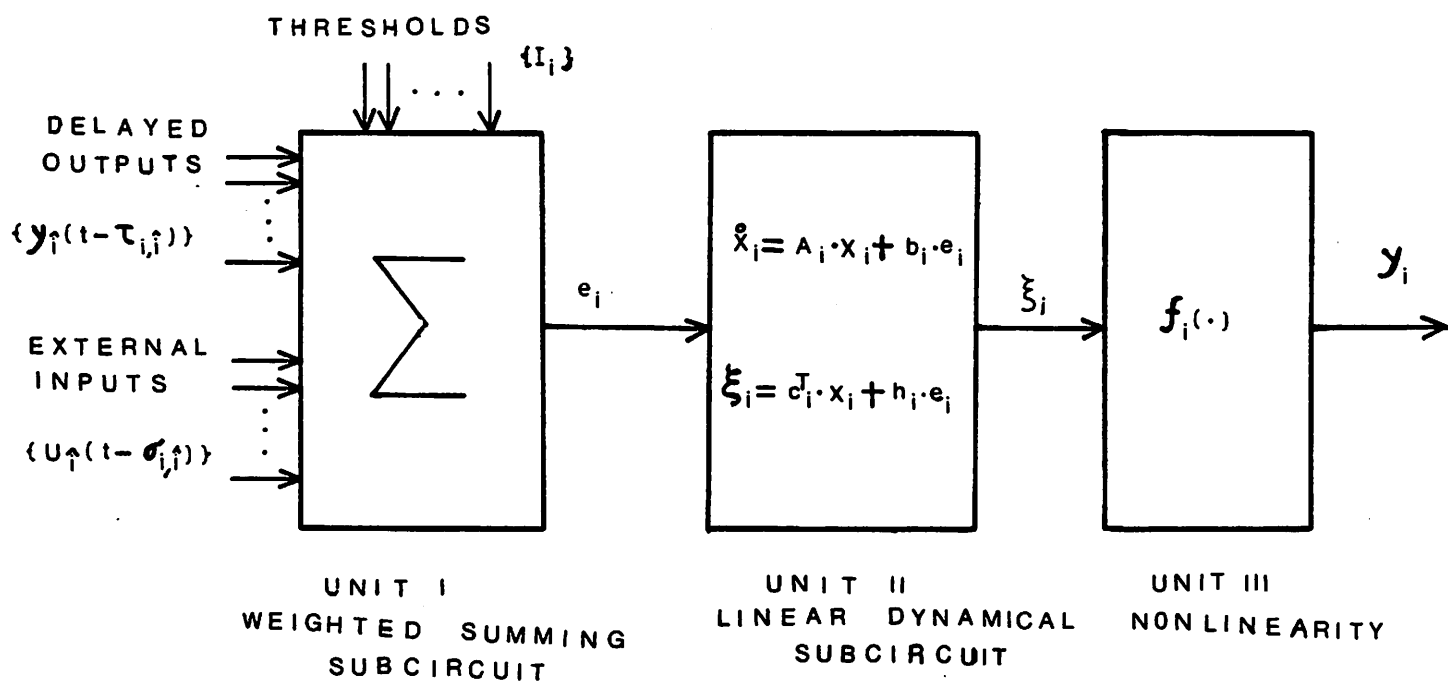(c)
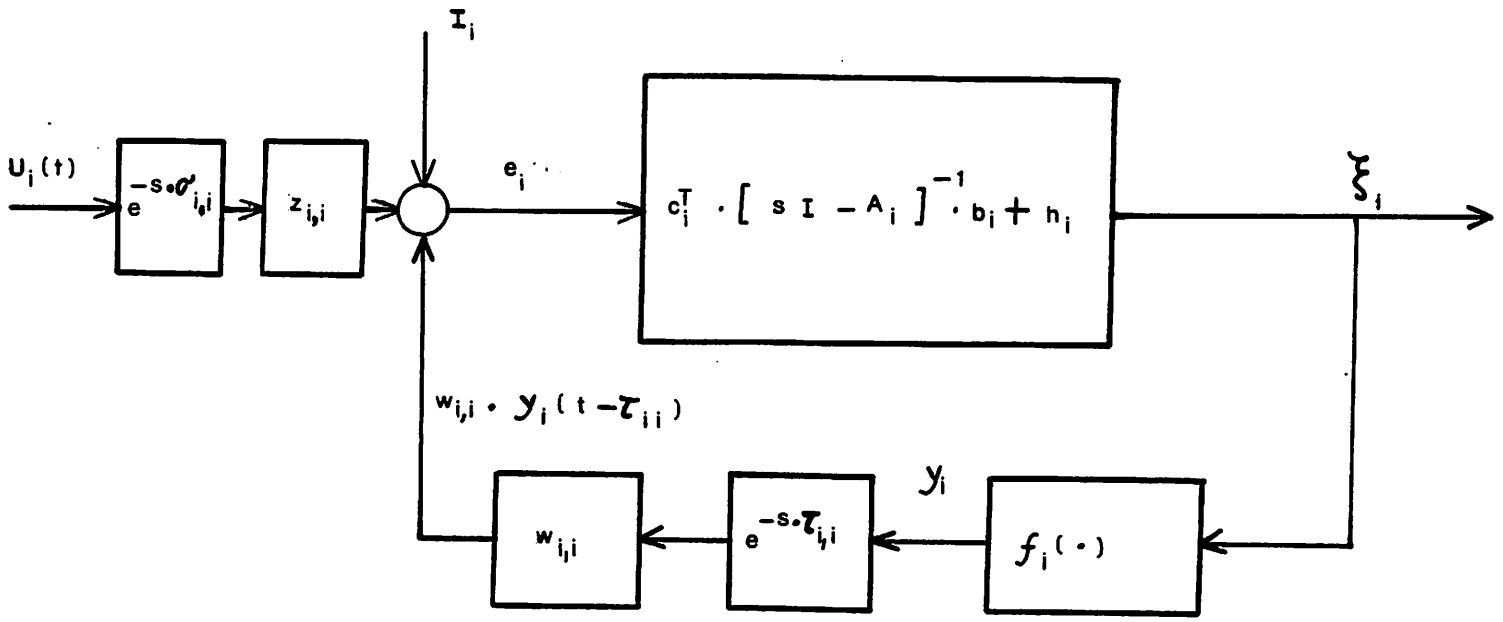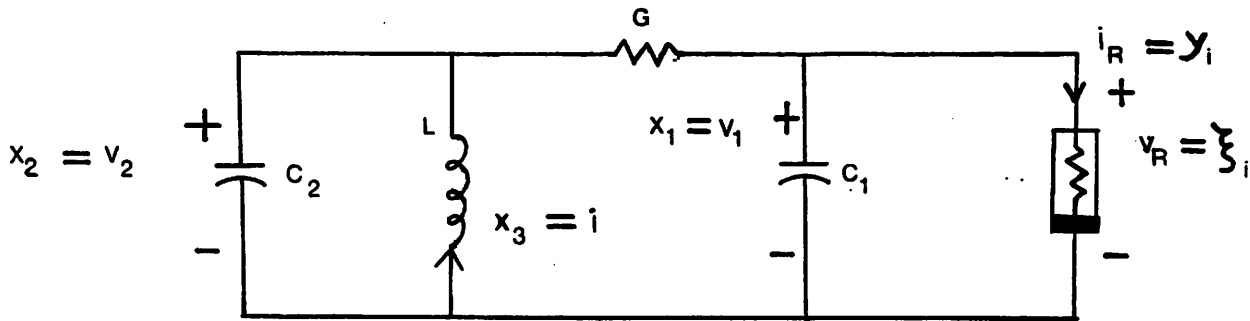
FIGURE 2

(a)

(b)

(c)

F I G U R E 3

(a)

(b)

FIGURE 4

THRESHOLDS

$\{I_i\}$

DELAYED
OUTPUTS

$\{y_i(t-\tau_{i,i})\}$

EXTERNAL
INPUTS

$\{U_i(t-\sigma_{i,i})\}$

$\sum$

e_i

$\dot{x}_i = A_i \cdot x_i + b_i \cdot e_i$

$\xi_i = c_i^T \cdot x_i + h_i \cdot e_i$

ξ_i

$f_i(\cdot)$

y_i

UNIT I
WEIGHTED SUMMING
SUBCIRCUIT

UNIT II
LINEAR DYNAMICAL
SUBCIRCUIT

UNIT III
NONLINEARITY

FIGURE 5

FIGURE 6

$x_2 = v_2$

$+$

C_2

$-$

L

$x_3 = i$

G

$x_1 = v_1$

$+$

C_1

$-$

$i_R = y_i$

$+$

$v_R = \xi_i$

$-$

(a)

$i_R = f_i(v_R)$

m_0

-1

1

v_R

m_1

m_0
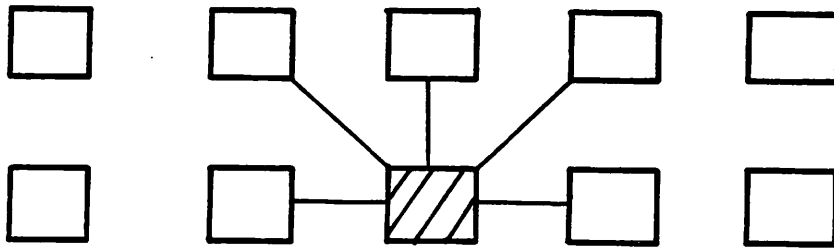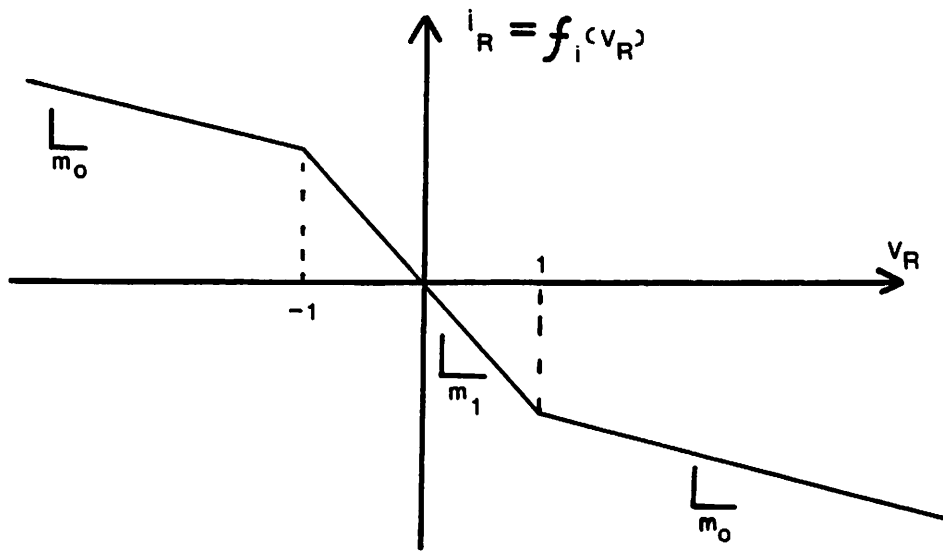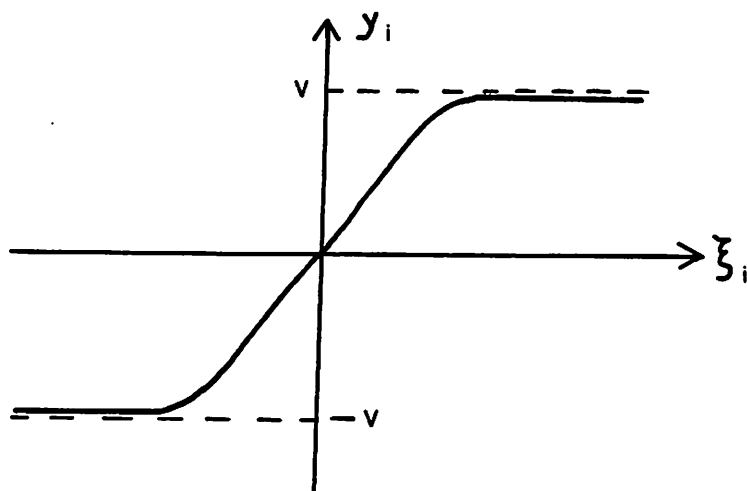
(b)

FIGURE 7

FIGURE 8

FIGURE 9

$$-A \qquad O \qquad A$$
$$w_{i,i}$$
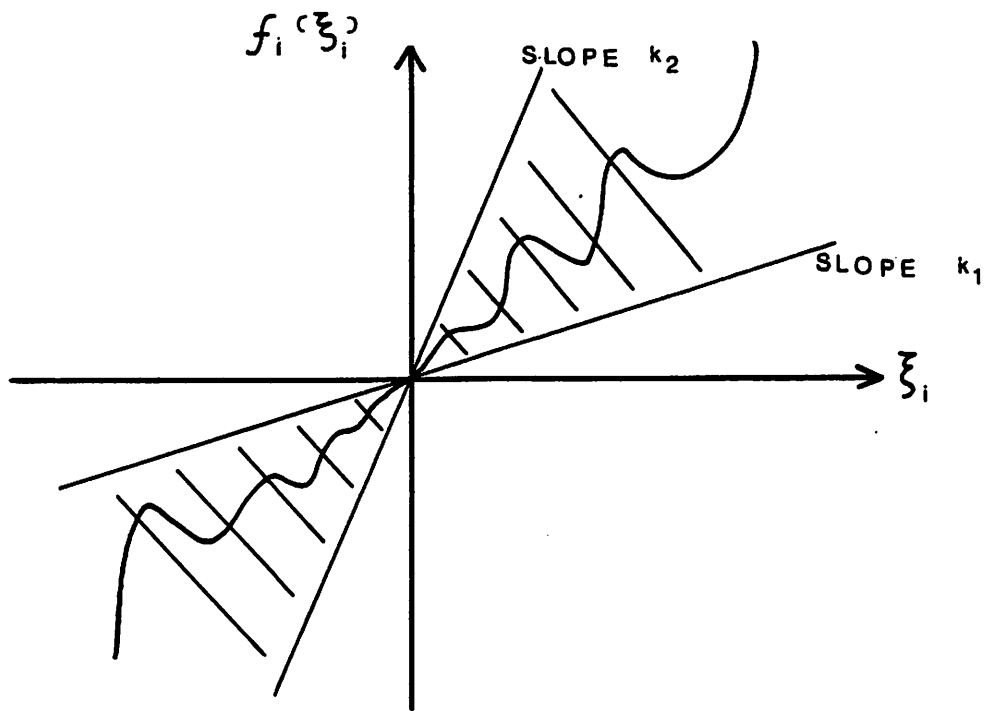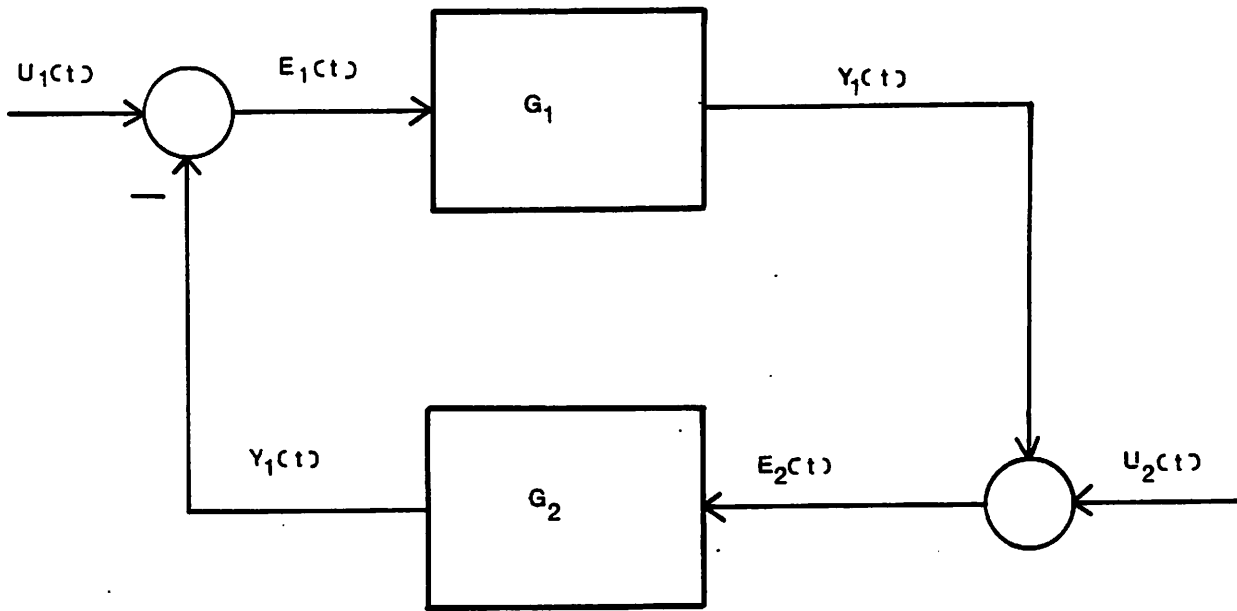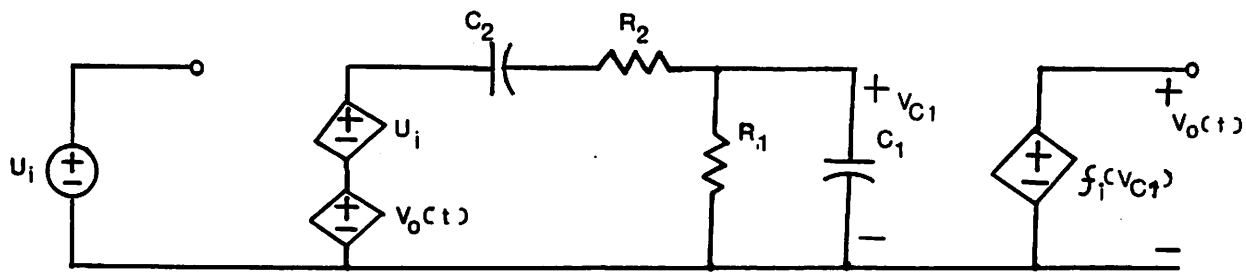
FIGURE 10

(a)
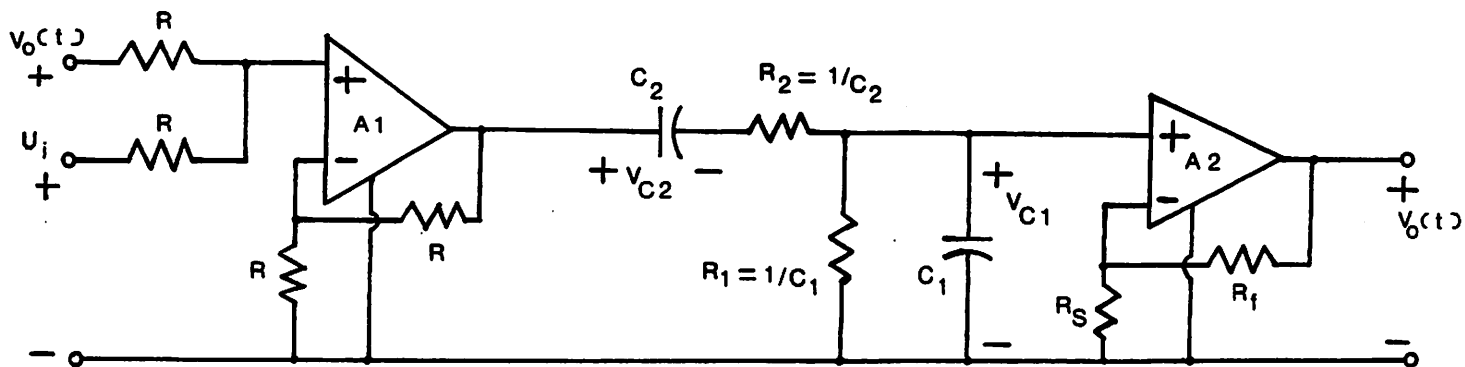
(b)

(c)

FIGURE 11

FIGURE 12

FIGURE 13